

Entanglement and apparent thermality in simulated black holes

Iason A. Sofos, Andrew Hallam, and Jiannis K. Pachos
School of Physics and Astronomy, University of Leeds, Leeds LS2 9JT, UK
(Dated: March 16, 2026)

We investigate the apparent thermality of Hawking radiation in the semi-classical limit of quantum black holes using the mean-field limit of a chiral spin-chain simulator, which models fermions propagating on a black hole space-time in the continuum. In this free-theory regime, no genuine thermalisation occurs. Nevertheless, we show that a bipartition across the event horizon yields a reduced density matrix whose mode occupations follow an apparent thermal Fermi–Dirac distribution. In contrast, partitions away from the horizon do not exhibit such thermal distributions, reflecting the absence of thermal behaviour. Our results demonstrate that Hawking radiation appears thermal only with respect to horizon bipartitions in free theories, whilst genuine thermal behaviour emerges only in the presence of interactions deep in the black hole interior.

I. Introduction

The theoretical study of quantum black holes has revealed a deep relationship between general relativity, thermodynamics, and quantum field theory [1]. By viewing the entropy of a black hole as a measure of how much information the event horizon obscures from an external observer, Bekenstein [2, 3] argued that it was natural to associate a black hole with a physical entropy. The physical equivalence between the laws of black hole mechanics and thermodynamics was solidified when Hawking demonstrated that the vacuum state of the space-time containing a black hole is a thermal state with a well-defined temperature known as the Hawking temperature, T_H [4–6]. This is the Hawking effect, and it is derived by analysing the semi-classical behaviour of quantum fields in a space-time containing a black hole.

Despite theoretical advancements in the study of quantum black holes, there remains several fundamental open questions, including whether, via black hole formation and evaporation, information of the black hole’s internal content is erased (the black hole information paradox) [7, 8]; why black hole entropy appears to be independent of the number of quantum fields [9–11]; what quantum degrees of freedom can be attributed to black hole entropy [12, 13]. In an effort to illuminate our understanding of these questions, there have been significant efforts, theoretically and, more recently, experimentally [14–21], towards realising physical analogues of black holes. Such a system was first proposed by Unruh, who argued that sonic analogues of black holes would experience a process analogous to the Hawking effect [22, 23]. Since then, a myriad of systems have been proposed to simulate not only the physics of black holes but also cosmological inflation, the early universe, and aspects of the standard model [24–28].

Here, we consider a chiral spin-chain model [29–32] that, in its continuum limit, due to the emergence of an effective Lorentz invariance in its low-energy limit, describes a theory of non-interacting Dirac fermions in a curved space-time geometry. This Lorentz invariance is naturally broken at the length scales of the spin-chain’s lattice spacing as a consequence of the model’s non-linear

dispersion relation. We calculate the density of states of the fermion zero-modes in various sub-regions of the space-time describing a (1+1)-dimensional black hole, which is finite as a consequence of the non-linear dispersion relation [26–28, 33–37]. By assuming that the fermions inside the black hole are well described by a thermal state at the Hawking temperature, the density of states can be used to compute the entropy of the fermion zero-modes across different regions of the black hole space-time. This includes the interior, where the entropy diverges logarithmically as the lattice spacing approaches zero [38–40], as well as the exterior.

In parallel, we employ numerical simulations to investigate the entanglement entropy of the chiral spin-chain following a bipartition of the lattice into two subsystems. Generally, we expect that the entropy of the fermion zero-modes agrees with the entanglement entropy of the chiral spin-chain if the state describing the partitioned system is thermal, as, in this case, the von Neumann entropy is equivalent to the thermodynamic entropy of the subsystem’s microstates [13, 41]. When the system is partitioned at the event horizon, we find that the entanglement entropy is well described by the analytic fermion zero-mode entropy of the black hole’s interior, suggesting that the ground state of the partitioned system is thermal. However, when the system is partitioned further from the horizon, we find that this agreement breaks down, indicating that the subsystem’s ground state appears thermal only when partitioned near the event horizon [42, 43]. We verify this by studying the subsystem’s mode occupation, which reveals a thermal Fermi–Dirac distribution only for horizon partitions. This breakdown of thermality for arbitrary partitions indicates that no genuine thermalisation occurs in the free-theory regime, implying that the simulated black hole’s information is not entirely erased [44].

To extract the Hawking temperature from the entanglement spectrum, it is necessary to transform the mean-field Hamiltonian into a form with only nearest-neighbour interactions and a linear coupling profile. In this form, the Hamiltonian’s continuum limit approximates both the entanglement Hamiltonian and the Dirac Hamiltonian near the event horizon. In the continuum

limit, this transformation corresponds to a change of coordinates that preserves the curvature of the underlying space-time; thus, the physical value of the Hawking temperature remains invariant.

II. Lattice simulator of Dirac fermions in black hole background

In this section, we introduce the chiral spin-chain model [29–32], for which, due to the emergence of an effective Lorentz invariance at low energies, the continuum limit Hamiltonian is described by that of massless Dirac fermions propagating on a (1 + 1)-dimensional curved space-time geometry. Thus, by simulating the chiral spin-chain Hamiltonian, we can probe the entropy and thermality of fermions on a black hole space-time.

The chiral spin-chain model, which describes a one-dimensional chain of N interacting spin-1/2 spins, is defined by the Hamiltonian [29–32]

$$H = \sum_{n=1}^N \left[-\frac{u}{2} (\sigma_n^x \sigma_{n+1}^x + \sigma_n^y \sigma_{n+1}^y) + \frac{v}{4} \chi_n \right], \quad (1)$$

where $u, v \in \mathbb{R}$, $\{\sigma_n^x, \sigma_n^y, \sigma_n^z\}$ are the Pauli matrices acting on the n th spin, $\chi_n = \boldsymbol{\sigma}_n \cdot (\boldsymbol{\sigma}_{n+1} \times \boldsymbol{\sigma}_{n+2})$ is a spin chirality operator [45, 46], and $\boldsymbol{\sigma}_n = (\sigma_n^x, \sigma_n^y, \sigma_n^z)$.

Obtaining the continuum limit of the chiral spin-chain begins with a Jordan-Wigner transformation, which maps the spins to a system of interacting fermions. For the analysis considered in the present work, we assume weak fluctuations, so a mean-field theory approximation can be applied. This transforms the chiral spin-chain Hamiltonian of Eq. (1) to the free fermion Hamiltonian [29–32]

$$H_{MF} = \sum_{n=1}^N \left(-uc_n^\dagger c_{n+1} - \frac{iv}{2} c_n^\dagger c_{n+2} \right) + \text{H.c.}, \quad (2)$$

where c_n^\dagger and c_n are fermionic creation and annihilation operators, respectively, satisfying the anti-commutation relations $\{c_n, c_m^\dagger\} = \delta_{nm}$ and $\{c_n, c_m\} = \{c_n^\dagger, c_m^\dagger\} = 0$.

By re-labelling the lattice sites such that they alternate between two sub-lattices, A and B , and introducing a two-site unit cell, as illustrated in Fig. 1, the mean-field Hamiltonian of Eq. (2) can, following a Fourier transform, be expressed as [29–32]

$$H_{MF} = \sum_p \chi_p^\dagger h(p) \chi_p, \quad (3)$$

where $\chi_p = (a_p, b_p)^T$ is a two-component spinor and

$$h(p) = \begin{pmatrix} g(p) & f(p) \\ f^*(p) & g(p) \end{pmatrix}, \quad (4)$$

where $f(p) = -u(1 + e^{-iacp})$ and $g(p) = v \sin(acp)$, is a single-particle Hamiltonian that can be diagonalised to

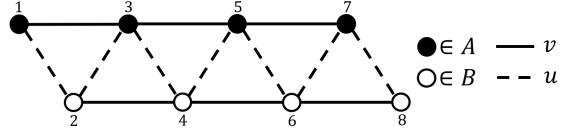


Figure 1. Schematic of the lattice corresponding to the chiral spin-chain model Hamiltonian of Eq. (1), where the lattice sites alternate between two sub-lattices, A and B , and a two-site unit cell has been introduced.

obtain the following dispersion relation: [29–32]

$$E(p) = v \sin(acp) \pm 2u \cos(acp/2), \quad (5)$$

which has Fermi points located at momenta $p_0 = \frac{\pi}{ac}$ and $p_{\pm} = \pm \frac{1}{ac} \arccos\left(1 - \frac{2u^2}{v^2}\right)$, the latter of which exist only in the regime where $v^2 > u^2$. In Fig. 2, we see that the dispersion relation possesses Dirac cones that are tilted by the coupling v , resulting in the emergence of these Fermi points when these cones over-tilt [29–32].

The low-energy limit of the mean-field theory can be taken by Taylor expanding the single-particle Hamiltonian of Eq. (4) around the Fermi point p_0 to $O(p)$. Doing so gives

$$h(p + p_0) = -a_c v \not{p} + a_c u \sigma^y p \equiv e_a^x \alpha^a p, \quad (6)$$

where the coefficients $e_0^x = -a_c v$ and $e_1^x = a_c u$ along with the matrices $\alpha^0 = \mathbb{1}$ and $\alpha^1 = \sigma^y$ have been defined, and $a \in \{0, 1\}$. Following this, the continuum limit $a_c \rightarrow 0$ and the thermodynamics limit $N_c \rightarrow \infty$ can be taken, whilst renormalising the couplings $a_c u \rightarrow u$ and $a_c v \rightarrow v$ and defining the spatial coordinate $x = na_c$ in the process. Thus, in this continuum and low-energy limit, the mean-field Hamiltonian of Eq. (3) is given by [29–32]

$$H_{MF} = \int dp \chi^\dagger(p) e_a^x \alpha^a p \chi(p). \quad (7)$$

Finally, by performing a Fourier transform of the Hamiltonian of Eq. (7) into real space, then a Legendre transformation, the following action S can be obtained:

$$S = i \int d^{1+1}x |e| \bar{\psi}(x) e_a^\mu \gamma^a \overleftrightarrow{\partial}_\mu \psi(x), \quad (8)$$

where $A \overleftrightarrow{\partial}_\mu B = \frac{1}{2}(A \partial_\mu B - (\partial_\mu A) B)$, the coefficients $e_0^t = 1$ and $e_1^t = 1$, the flat space-time gamma matrices $\gamma^a = \sigma^z \alpha^a$, and the conjugate spinor $\bar{\psi}(x) = \psi^\dagger(x) \gamma^0$ have been defined, $|e| = \det(e_a^\mu)$, and $\mu \in \{t, x\}$ [29–32].

The action of Eq. (8) is that of a massless Dirac spinor ψ on a (1+1)-dimensional Riemann-Cartan space-time, with the curved space-time spinor ψ being related to the lattice spinor χ via the renormalisation $\chi = \sqrt{|e|} \psi$ and the zweibein being given by [29–32]

$$e_\mu^a = \begin{pmatrix} 1 & v/u \\ 0 & 1/u \end{pmatrix}, \quad e_a^\mu = \begin{pmatrix} 1 & -v \\ 0 & u \end{pmatrix}, \quad (9)$$

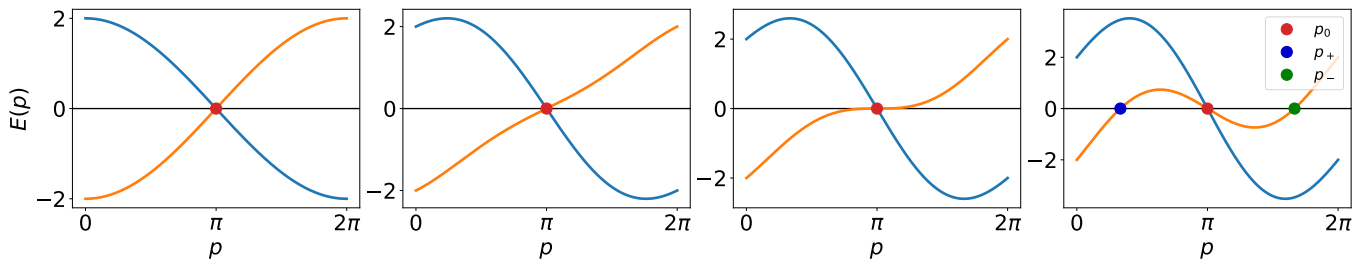


Figure 2. Blue and orange curves show the positive and negative mean-field dispersion relations of Eq. (5), respectively, for fixed $u = 1$ and various coupling strengths v (from left to right, $v = 0, 0.5, 1, 2$). As the coupling v increases, the Dirac cone about the Fermi point p_0 tilts. At the critical point $u^2 = v^2$, which corresponds to the event horizon, the cone over-tilts, resulting in the emergence of two further Fermi points p_{\pm} .

which correspond to the following space-time metric line element:

$$ds^2 = \left(1 - \frac{v^2}{u^2}\right) dt^2 - \frac{2v}{u^2} dt dx - \frac{1}{u^2} dx^2. \quad (10)$$

It can be verified from the lattice spinor's anti-commutation relations and the zweibein of Eq. (9) that the curved space-time spinor satisfies the necessary anti-commutation relations of Eq. (A.20).

If the couplings v and u are slowly varying position-dependent functions $v(x)$ and $u(x)$, then the line element of Eq. (10) is that of the (1+1)-dimensional Gullstrand-Painlevé metric [47, 48], which describes the space-time geometry of a (1+1)-dimensional black hole when the surface gravity κ of the metric is positive, and a white hole when it is negative [26, 27] (see Appendix B.1). The Gullstrand-Painlevé metric does not possess a coordinate singularity at the event horizon, which is located at $v(x_h)^2 = u(x_h)^2$, and is therefore valid in both the interior and exterior space-time of the black/white hole, with the region bounded by $v(x)^2 \geq u(x)^2$ corresponding to the interior [29, 30]. Though the Gullstrand-Painlevé metric is not *static* (not invariant under the time-reversal transformation $t \mapsto -t$), it is *stationary* (invariant under the time-translation transformation $t \mapsto t + t_0$). As the metric is stationary, it admits a time-like Killing vector $\xi^\mu = \delta_t^\mu$ (equivalently denoted ∂_t), which allows energy to be well-defined in the black hole's interior region and conserved along the metric's geodesics [26–28] (see Appendix A).

It was demonstrated in Refs. [30, 49] that a single-particle state initially localised in the region corresponding to the black hole's interior, which evolves unitarily under the mean-field Hamiltonian of Eq. (2), undergoes scattering across the event horizon that causes it to thermalise with a temperature given by T_H . The propagation of the single-particle state across the event horizon, which occurs due to mean-field theory's non-linear dispersion relation [26–28, 33–37], is analogous to the quantum tunnelling interpretation of Hawking radiation [50].

III. Entropy of simulated (1+1)D Dirac fermions in black hole background

In this section, we derive analytic expressions for the entropy of the fermion zero-modes in the interior and exterior regions of a (1+1)-dimensional black hole. Two assumptions, that the state describing the fermions in the black hole's interior region is approximately thermal (that is, well described by a Gibbs state), and that the temperature of this state is the Hawking temperature, are key to this derivation. The derivation utilises a non-linear dispersion relation to find a finite density of states of the fermion zero-modes, which, in turn, can be used along with the assumptions of thermality to obtain their thermal energy and, hence, thermodynamic entropy. Under this assumption of thermality, we expect that the thermodynamic entropy of these fermion zero-modes is equivalent to the entanglement entropy associated with the bipartitioning of space-time by the event horizon [13, 41]. In Sec. IV, where numerical simulations of the chiral spin-chain's entanglement entropy are employed, this equivalence will be used to probe the thermality of the black hole.

In the mean-field description, the ground state corresponds to a filled Fermi sea with all negative-energy single-particle modes occupied. Fluctuations around this state are described by particles with positive energy and by antiparticles realised as holes created by removing fermions from the occupied negative energy states. Hence, in the low-temperature regime, the thermodynamic behaviour will be determined by excitations near the Fermi energy $E(p) = 0$. The density of states $N(0)$, at zero energy, of the fermion zero-modes enclosed in a sub-region of length s of the black hole's interior will be given by [26, 27]

$$N(0) = \frac{N_F}{2\pi\hbar} \int_{a_c}^s dx \int_{\mathbb{R}} dp \delta(E(p)), \quad (11)$$

where $E(p)$ is the dispersion relation of the fermions and N_F denotes the integer number of massless fermion fields.

As the effective Lorentz invariance emerges in the low-energy limit of the chiral spin-chain's continuum limit, we

can identify the mean-field dispersion relation of Eq. (5) as an appropriate dispersion relation for the fermions in the black hole space-time. Moreover, as the continuum limit is defined microscopically on a lattice, the lattice spacing provides a natural ultraviolet cut-off that prevents the density of states of Eq. (11) from being divergent. Operationally, this enters in two equivalent ways: First, the spatial integral should not be extended to separations smaller than a_c from the event horizon x_h and the coordinate origin $x = 0$; that is, $a_c \leq s \leq x_h - a_c$ [51]. This prevents an infinite number of degrees of freedom, from points on either side of the horizon or the coordinate origin, from contributing to the density of states [38, 51, 52]. Second, as the mean-field dispersion relation is non-linear, it breaks the effective Lorentz invariance at

distances comparable to the lattice spacing [26–28, 33–37]. This allows for the density of states to be finite, as, by introducing a fundamental length scale, it prevents the localisation of an infinite number of degrees of freedom into an arbitrarily small volume [38, 51, 52].

In the regime corresponding to the black hole’s interior, the mean-field dispersion relation has three zero-modes, all of which are sub-luminal in nature (those of the negative solution of Eq. (5)) when u and v are of the same sign. Thus, taking the sub-luminal mean-field dispersion relation, and making use of the Dirac delta identity $\delta(f(x)) = \sum_i \delta(x - x_i)/|f'(x_i)|$, the density of states of Eq. (11) for the fermion zero-modes enclosed in the interior region of the black hole can be expressed as

$$N(0) = \frac{N_F}{2\pi\hbar} \int_{a_c}^s dx \left(\frac{1}{|1 - v(x)|} + \left| \frac{1}{(1 - v(x))} - \frac{1}{(1 + v(x))} \right| \right), \quad (12)$$

where the couplings have been renormalised and we have taken $u = 1$, which can be solved for a given coupling $v(x)$ to obtain the relevant density of states. Here, we take the coupling $v(x) = \sqrt{x_h/x}$, which corresponds to that of a Schwarzschild black hole [26, 27]. For this coupling, the density of states of Eq. (12) can be solved to yield

$$N(0) = \frac{N_F x_h}{\pi\hbar} \left(\ln \left| \frac{s^{\frac{1}{2}} + x_h^{\frac{1}{2}}}{s^{\frac{1}{2}} - x_h^{\frac{1}{2}}} \right| + \ln \left| \frac{x_h^{\frac{1}{2}}}{s^{\frac{1}{2}} - x_h^{\frac{1}{2}}} \right| - \frac{1}{2} \left(\frac{s}{x_h} \right) - 3 \left(\frac{s}{x_h} \right)^{\frac{1}{2}} \right). \quad (13)$$

Assuming that the reduced state associated with the fermions in the black hole’s interior is well described by a thermal Gibbs state, the density of states can be used to find the thermal energy $\mathcal{E}(T)$ and, hence, the thermodynamic entropy $\mathcal{S}(T)$ of the fermions in the interior region of the black hole. The thermal energy of the fermions in the black hole’s interior will be given by [26–28]

$$\mathcal{E}(T) = N(0) \int_0^\infty dE \frac{E}{e^{E/T} + 1}, \quad (14)$$

which can be solved using the change of variables $u = -E/T$ and the dilogarithmic identity $\text{Li}_2(1) = \pi^2/6$ [53, 54] to give [26–28]

$$\mathcal{E}(T) = \frac{\pi^2}{6} N(0) T^2, \quad (15)$$

where T is the temperature at which the fermions are in equilibrium. Using the first law of thermodynamics, $d\mathcal{E}(T) = T d\mathcal{S}(T)$, the entropy of the fermion zero-modes in the black hole’s interior can be found to be

$$\mathcal{S}(T) = \frac{\pi^2}{3} N(0) T. \quad (16)$$

Assuming that, in addition to being described by a thermal state, and as semi-classical intuition suggests, the temperature of this thermal state is equal to the Hawking temperature [5, 6]

$$T_H = \frac{\hbar\kappa}{2\pi} = \frac{\hbar}{4\pi x_h}, \quad (17)$$

where $\kappa = -v'(x_h)$ is the surface gravity of the Gullstrand-Painlevé metric (see Appendix B.1), the fermion zero-mode entropy of the black hole’s interior region will be

$$\mathcal{S}(T_H) = \frac{N_F}{12} \left(\ln \left| \frac{s^{\frac{1}{2}} + x_h^{\frac{1}{2}}}{s^{\frac{1}{2}} - x_h^{\frac{1}{2}}} \right| + \ln \left| \frac{x_h^{\frac{1}{2}}}{s^{\frac{1}{2}} - x_h^{\frac{1}{2}}} \right| - \frac{1}{2} \left(\frac{s}{x_h} \right) - 3 \left(\frac{s}{x_h} \right)^{\frac{1}{2}} \right). \quad (18)$$

Taking the length s of the black hole’s interior region to

be $s = x_h - a_c$, such that the fermion zero-mode entropy

of this region corresponds to that of the entire black hole, and working in the limit $0 < a_c \ll x_h$, Eq. (18) for the fermion zero-mode entropy of the black hole's interior reduces to

$$\mathcal{S}(T_H) = \frac{N_F}{6} \ln\left(\frac{2x_h}{a_c}\right) + \mathcal{S}_0, \quad (19)$$

where $\mathcal{S}_0 = N_F(2 \ln(2) - 7)/24$, which is logarithmically divergent with the lattice constant a_c .

The logarithmically divergent part of Eq. (19) for the black hole's fermion zero-mode entropy can be made identical to the Bekenstein-Hawking entropy $S_{BH} = A_{bh}/4l_p^2$, where $A_{bh} = 2$ for a (1+1)-dimensional black hole, if we impose that the effective Planck length squared l_p^2 is given by

$$\frac{1}{l_p^2} = \frac{1}{\hbar G_{\text{eff}}} = \frac{N_F}{3} \ln\left(\frac{2x_h}{a_c}\right). \quad (20)$$

This is equivalent to the renormalisation of the effective gravitational constant G_{eff} , which has been suggested [9, 10] as a method for renormalising the divergences arising in the derivation of the Bekenstein-Hawking entropy from a statistical mechanics, or entanglement entropy, approach [9, 10, 37]. This renormalisation is also a necessary procedure for removing the black hole entropy's dependence on the number of fermion species

[9–11], which is required as Bekenstein-Hawking entropy depends solely on the black hole's surface area and the gravitational constant.

In addition to studying the fermion zero-mode entropy of the black hole's interior, we can extend this analysis to derive an expression for the fermion zero-mode entropy of both the black hole's interior and exterior regions. The method of this derivation is analogous to that of the black hole's interior, and so, for brevity, we leave the details of this derivation to Appendix C. It involves determining the density of states of Eq. (12) for both the interior region, which is bound by $[a_c, x_h - a_c]$, and a portion of the exterior space-time, which we take to be bound by $[x_h + a_c, s]$, where $s \geq x_h + a_c$ is the distance from the coordinate origin $x = 0$. Here, as before, the lower limit of s has been restricted to a distance a_c from the event horizon to prevent degrees of freedom of points on either side of the event horizon with a separation of less than a_c from contributing to the density of states and entropy. In contrast to before, only the zero-mode corresponding to the Fermi point at p_0 will contribute to the density of states in the exterior region. Considering this, and once again assuming that the reduced state describing the fermions in the black hole's interior is suitably described by a thermal Gibbs state with a temperature T_H , the fermions' thermal energy and thermodynamic entropy can be defined, the latter of which can be solved to yield

$$\mathcal{S}(T_H) = \frac{N_F}{6} \ln\left(\frac{2x_h}{a_c}\right) + \frac{\tilde{N}_F}{12} \left(\frac{1}{2} \left(\frac{s}{x_h} \right) + \left(\frac{s}{x_h} \right)^{\frac{1}{2}} + \ln\left(\frac{2x_h^{\frac{1}{2}}}{a_c}\right) + \ln\left|s^{\frac{1}{2}} - x_h^{\frac{1}{2}}\right| \right) + \mathcal{S}'_0 \quad (21)$$

in the limit $0 < a_c \ll x_h$, where \tilde{N}_F denotes the integer number of massless fermionic fields in the black hole space-time's exterior region and $\mathcal{S}'_0 = \mathcal{S}_0 - 3\tilde{N}_F/24$.

IV. Entanglement entropy of chiral spin-chain simulator

In the previous section, having assumed that the interior region is well described by a thermal state, we derived analytic expressions for the fermion zero-mode entropy for various regions of the black hole's space-time. We now numerically compute the entanglement entropy of the chiral spin-chain for arbitrary bipartitions. We do this for two distinct cases: first, when the partition is located at the event horizon; and second, when the partition is located at a lattice site in the region corresponding to the black hole's interior or exterior. We expect that the fermion zero-mode entropy agrees with the entanglement entropy if the ground state of the partitioned system is thermal, as, in this case, the von Neumann

entropy equates to the thermodynamic entropy of the subsystem's microstates (fermion zero-modes) [13, 41]. Thus, by comparing our analytic predictions and numerical results, we can identify the regimes where this equality and, by extension, the assumption of thermality is valid, and where it breaks down. We will see that as the system is free, the thermality condition is generally not valid, as, due to the absence of interactions, the system cannot truly thermalise. Surprisingly, this equality holds only when partitioning at the event horizon, due to the unique physics emerging in that region [5, 6].

Consider a quantum system that is bipartitioned into two subsystems, \mathcal{A} and \mathcal{B} , as illustrated in Fig. 3a, with a ground state $|\psi_{AB}\rangle \in \mathcal{H}_A \otimes \mathcal{H}_B$ described by the density matrix $\rho_{AB} = |\psi_{AB}\rangle\langle\psi_{AB}|$, where \mathcal{H}_A and \mathcal{H}_B denote the Hilbert spaces of \mathcal{A} and \mathcal{B} , respectively. The bipartite entanglement entropy S_A of subsystem \mathcal{A} , which quantifies the correlations between \mathcal{A} and \mathcal{B} , is defined as $S_A = -\text{Tr}(\rho_A \ln(\rho_A))$, where $\rho_A = \text{Tr}_B(\rho_{AB}) = \sum_i \langle i_B | \rho_{AB} | i_B \rangle$ denotes the reduced density matrix of \mathcal{A} and $\{|i_B\rangle\} \in \mathcal{H}_B$ the orthonormal basis of \mathcal{H}_B .

We take the Hamiltonian of Eq. (2) with couplings

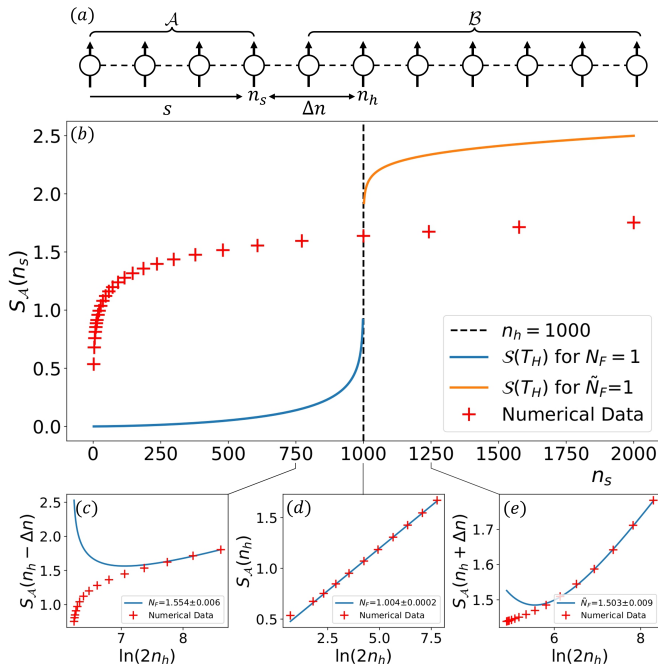


Figure 3. (a) Schematic of spin-chain bipartition at lattice site n_s located a distance Δn from n_h . (b) Red data points show entanglement entropy $S_{\mathcal{A}}(n_s)$ of \mathcal{A} as a function of the partition site n_s for a system with $n_h = 1000$. Blue and orange curves show the fermion zero-mode entropies of Eqs. (18) and (21) for the black hole space-time’s interior and exterior regions, respectively, with $N_F = \tilde{N}_F = 1$ and the non-universal constant of the exterior region chosen to match that obtained for the horizon partition. (c), (d), and (e) Red data points show the entanglement entropy $S_{\mathcal{A}}(n_s)$ of \mathcal{A} as a function of the partition’s location, where the system is partitioned at $n_s = n_h - \Delta n$ (interior), the event horizon n_h , and $n_s = n_h + \Delta n$ (exterior), respectively, with $\Delta n = 250$. Blue curves show data interpolated using Eqs.(18), (19), and (21) for the fermion zero-modes’ entropy for the interior, horizon, and exterior regions of the black hole space-time, respectively. To avoid partitioning the two-site unit cell of the continuum limit, only even n_h were considered. For all figures, systems of $N = 10000$ lattice sites with couplings $v(n) = \sqrt{n_h/n}$ and $u = 1$ were taken.

$v(n) = \sqrt{n_h/n}$ and $u = 1$, which represent the Schwarzschild black hole profile, where we have introduced the discrete spatial coordinate $n = x/2a$ and $a = a_c/2 = 1/N$ is the chiral spin-chain’s lattice spacing. Moreover, n_h is the lattice site where the event horizon is located, defined as the site for which $v(n_h) = 1$. As the Hamiltonian of Eq. (2) is that of a free fermion system, the entanglement entropy can be efficiently computed via

$$S_{\mathcal{A}} = - \sum_i (\lambda_i \ln(\lambda_i) + (1 - \lambda_i) \ln(1 - \lambda_i)), \quad (22)$$

where λ_i denotes the eigenvalues of the two-point correlation function $C_{ij} = \langle P_{\mathcal{A}} \phi_j | P_{\mathcal{A}} \phi_i \rangle$, $|P_{\mathcal{A}} \phi_i\rangle$ is the projection of the single-particle Hamiltonian’s negative energy eigenstates onto \mathcal{A} , and $i, j \in \{1, \dots, N\}$ [55, 56]. The

entanglement entropy of this system with $N = 10000$ lattice sites and event horizon located at $n_h = 1000$ is given in Fig. 3b.

We now turn to the analytic expressions for the entropy given in Eqs. (18), (19), and (21), which correspond to partitions in the interior, at the horizon, and in the exterior regions of the black hole’s space-time, respectively, where we parametrise the partition’s location by the integer $n_s = s/2a$ that is an absolute distance $\Delta n \geq 2$ from n_h . In these formulas, the integer parameters N_F and \tilde{N}_F remain to be determined. To fix these parameters, we numerically evaluate the entanglement entropy for a fixed Δn as we vary the horizon’s position n_h and, hence, the partition n_s , as shown in Figs. 3c, d, and e. We find that, up to an overall additive constant, which is non-universal with respect to the chosen lattice parametrisation, only the expression corresponding to the horizon partition yields an integer value of $N_F \approx 1$, with this value converging as $N \rightarrow \infty$, whilst interior and exterior partitions suggest a larger value, both being in general non-integers. The convergence of $N_F \rightarrow 1$ in the thermodynamic limit, $N \rightarrow \infty$, for the horizon partition can be inferred from the entanglement entropy’s derivative, which, as shown in Fig. 4, plateaus around the value 1 for larger domains as the system size increases. In contrast to this, the deviation of N_F from an integer value as the partition moves from the horizon is emphasised in Fig. 4, where we plot its value from fitting the analytic formulas as n_h varies for different Δn ; we see that N_F is not a constant, in contradiction to the assumptions used to determine the fermion zero-mode entropy.

To illustrate the entropy for general partitions $n_s \neq n_h$, we adopt $N_F = 1$ for the interior and $\tilde{N}_F = 1$ for the exterior, reflecting the value of the number of fermionic fields determined for a horizon partition. Moreover, we fix the non-universal constant of the exterior region’s analytic zero-mode entropy to match the value obtained when partitioning at the horizon. As illustrated in Fig. 3b, we observe that the analytic zero-mode entropy formulas differ significantly from the numerically computed entanglement entropy in both the interior and exterior. Under the assumption of thermality, we expect the fermion zero-mode entropy to be equivalent to the entanglement entropy between the partitioned subsystems [13, 41]; thus, the increasing discrepancy between them as the partition deviates from the horizon signals the failure of thermality for general partitions. We also attribute the lack of consistent integer solutions for N_F and \tilde{N}_F to this breakdown of the assumed thermality that underpins the analytic derivations. In Sec. V, this is verified by studying the subsystem’s mode occupation, which reveals a Fermi-Dirac distribution only when the lattice is partitioned near the event horizon.

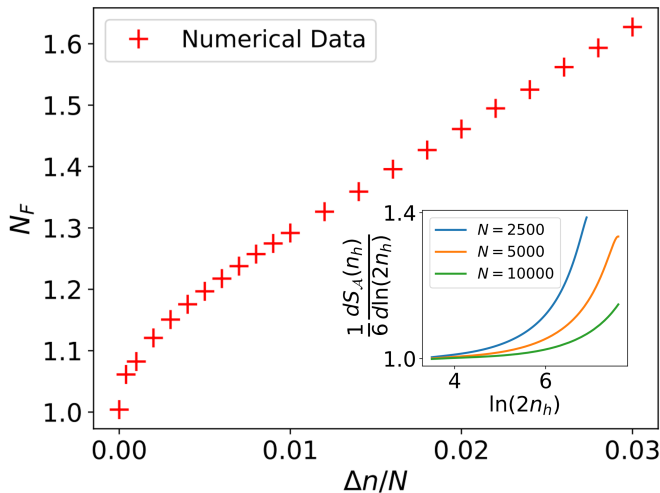


Figure 4. Data points show the interpolated value for the number of fermionic fields N_F as a function of the distance Δn of the partition $n_s = n_h - \Delta n$ from the event horizon n_h , for a system of $N = 10000$ lattice sites with couplings $v(n) = \sqrt{n_h/n}$ and $u = 1$. Each interpolated value of N_F is determined by fitting Eq. (18) to numerical data for the entanglement entropy for a fixed Δn as n_h is increased. The deviation from $N_F \approx 1$ as Δn increases indicates the breakdown of Eq. (18) for the fermion zero-mode entropy of the black hole's interior in describing the behaviour of the entanglement entropy as the partition deviates from the event horizon. Inset shows the derivative of the entanglement entropy $S_{\mathcal{A}}(n_h)$ with respect to $\ln(2n_h)$ following a horizon partition, $\Delta n = 0$, for increasing system sizes, indicating the regime where $N_F \approx 1$. As system size increases, the domain for which the gradient plateaus around 1 increases, suggesting that $N_F \rightarrow 1$ in the thermodynamic limit, $N \rightarrow \infty$.

V. Thermality of chiral spin-chain simulator

A. The breakdown of thermality

To further investigate the breakdown of thermality for non-horizon partitions, we examine the mode occupation expectation value, $\langle 0_M | c_k^\dagger c_k | 0_M \rangle$, of the mean-field Hamiltonian that simulates the black hole space-time with respect to the ground state $|0_M\rangle$ of the asymptotically flat Minkowski Hamiltonian (Eq. (2) with couplings $v = 0$ and $u = 1$). Here, c_k are the eigenmodes that diagonalise the mean-field Hamiltonian of Eq. (2) with the Gullstrand–Painlevé coupling profile $v(x) = \sqrt{x_h/x}$ and $u = 1$, which correspond to a black hole space-time. The mode occupation can be expressed as [57]

$$\langle 0_M | c_k^\dagger c_k | 0_M \rangle = \sum_{q: E_M < 0} |\langle E_{GP,k} | E_{M,q} \rangle|^2, \quad (23)$$

where $|E_{GP,k}\rangle$ and $|E_{M,k}\rangle$ denote the k th eigenstate of the single-particle Hamiltonians, h_{GP} and h_M , associated with H_{MF} for the Gullstrand–Painlevé and Minkowski coupling profiles, respectively. Their corresponding energy eigenvalues are denoted $E_{GP,k}$ and $E_{M,k}$. Evalu-

ating the mode occupation $\langle 0_M | c_k^\dagger c_k | 0_M \rangle$ is the lattice equivalent to determining the Minkowski vacuum expectation value perceived by an observer in a black hole space-time, which is the relevant quantity in the Unruh–Davies–Fulling and Hawking effects [57], and should not be interpreted as a dynamical quench.

To perform the partial trace of subsystem \mathcal{A} , we define the Gullstrand–Painlevé Hamiltonian only in the region corresponding to subsystem \mathcal{B} and take it to be zero elsewhere. This effectively traces out the degrees of freedom of \mathcal{A} . As illustrated in Fig. 5, when the system is partitioned at the event horizon ($\Delta n = 0$), the mode occupation expectation value of Eq. (23) follows a Fermi–Dirac distribution of the form

$$f(E_{GP,k}, T) = \frac{1}{e^{E_{GP,k}/T} + 1}, \quad (24)$$

where T is a free parameter representing temperature, indicating that the reduced state is indeed thermal. However, as the partition is shifted away from the horizon ($\Delta n \neq 0$), deviations from a Fermi–Dirac distribution appear and grow with increasing Δn . This behaviour is quantified in Fig. 6, which shows the integrated and absolute interpolation errors, $I(E_{GP,k})$ and $e(E_{GP,k})$, respectively, that arise when fitting the mode occupation data to a Fermi–Dirac distribution. In contrast to the horizon partition, where these errors decrease with system size, these errors grow as Δn increases, regardless of system size, confirming that the reduced state deviates progressively from thermal behaviour as the partition deviates from the horizon.

These findings support the conclusion that thermality, and thus the equivalence between statistical and entanglement entropy, holds only for partitions near the event horizon.

B. Thermality and the Hawking temperature

To extract an effective Hawking temperature from the simulated black hole system, the reduced density matrix describing the partitioned system's ground state must be equivalent to a thermal density matrix of finite temperature. This equivalence occurs when the mean-field Hamiltonian approximates the entanglement Hamiltonian of a free fermionic system, for which the eigenmode occupations follow a thermal Fermi–Dirac distribution with a well-defined temperature [58]. It was demonstrated in Ref. [57] that, in the continuum limit of free fermionic lattice systems with linear coupling strengths, the free fermion Hamiltonian approximates both the entanglement and Rindler Hamiltonian. In such cases, the effective temperature extracted from the mode occupation's Fermi–Dirac distribution is given by the Unruh temperature of the simulator, which coincides with the Hawking temperature near the event horizon.

We employ this method to probe the thermal properties of our chiral spin-chain simulator. However, the

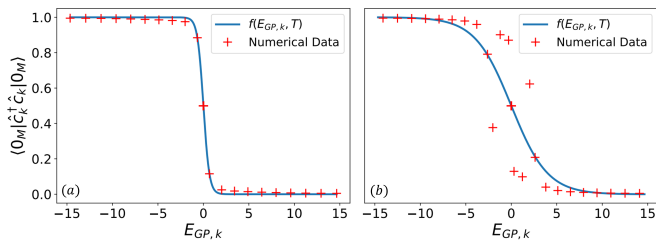


Figure 5. Red data points show the mode occupation expectation value $\langle 0_M | c_k^\dagger c_k | 0_M \rangle$ of the mean-field Hamiltonian that simulates the black hole space-time (Eq.(2) with the Gullstrand-Painlevé couplings $v(x) = \sqrt{x_h/x}$ and $u = 1$, defined only on \mathcal{B}) with respect to the ground state $|0_M\rangle$ of the Minkowski Hamiltonian (Eq. (2) with couplings $u = 1$ and $v = 0$, defined over the entire lattice) for a horizon partition ($\Delta n = 0$) and interior partition ($\Delta n = 50$), respectively. The abscissa shows the energy eigenvalues $E_{GP,k}$ of the single-particle Hamiltonian h_{GP} associated with H_{MF} for the Gullstrand-Painlevé couplings; for finite N the spectrum is bounded due to the lattice bandwidth. Blue curve shows data interpolated using the Fermi-Dirac distribution of Eq. (24) with $T = 0.3271$ and $T = 1.9237$, respectively. System sizes of $N = 2000$ lattice sites, with the horizon located at $n_h = 700$, were considered.

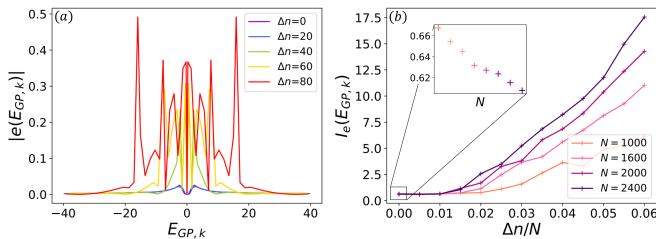


Figure 6. (a) Absolute value of interpolation errors $|e(E_{GP,k})|$ between the numerical and interpolated data for the mode occupation number $\langle 0_M | c_k^\dagger c_k | 0_M \rangle$, interpolated using a Fermi-Dirac distribution, for systems of increasing Δn with $N = 2000$ lattice sites. As Δn increases, and the system is partitioned further from n_h , increasing absolute interpolation errors indicate deviations from a Fermi-Dirac distribution in the mode occupation expectation value. (b) Integrated absolute interpolation errors $I_e(E_{GP,k})$ for increasing Δn and varied system sizes N , illustrating that the deviations from a Fermi-Dirac distribution as Δn is increased are not minimised at larger system sizes. This is in contrast to partitioning the system at n_h , where the integrated interpolation errors decrease with increasing system size. For both figures, systems with $n_h = N/4$ were considered.

mean-field Hamiltonian of Eq. (2) does not feature an overall linear coupling and, therefore, does not approximate the entanglement Hamiltonian required to extract a thermal spectrum. To address this, the mean-field Hamiltonian must be modified such that the black hole geometry is encoded with only a linear nearest-neighbour coupling $u(x)$. In the continuum limit, such a modification corresponds to performing a coordinate transformation from Gullstrand-Painlevé to Schwarzschild coordinates,

whilst preserving the space-time geometry (see Appendix D); thus, by mapping the black hole geometry to a mean-field Hamiltonian that approximates the entanglement Hamiltonian, the mode occupations of the partitioned ground state yields a Fermi-Dirac distribution from which T_H can be reliably extracted [57, 59]. This procedure fails, however, when the chirality term $v(x)$ is non-zero, as in this case the mean-field Hamiltonian no longer approximates the corresponding entanglement Hamiltonian.

Consider the mean-field Hamiltonian of Eq. (2) with a position-dependent nearest-neighbour coupling $u(x)$ and vanishing chirality term, $v(x) = 0$. In analogy with the chiral spin-chain, the low-energy continuum limit of this Hamiltonian corresponds to the action of a massless Dirac spinor on a $(1+1)$ D curved space-time; the resulting geometry is described by the line element [57, 60]

$$ds^2 = u(x)dt^2 - \frac{dx^2}{u(x)}, \quad (25)$$

which matches the Schwarzschild metric in $(1+1)$ dimensions. In particular, for the choice $u(x) = 1 - x_h/x$, this line element describes the exterior region of a Schwarzschild black hole with an event horizon located at x_h . This way, taking $v(x)$ to be zero and making $u(x)$ position dependent corresponds to a coordinate transformation from Gullstrand-Painlevé coordinates (t, x) to Schwarzschild coordinates (\tilde{t}, x) . Whilst the Hamiltonian's structure changes under this transformation, scalar quantities, such as the space-time curvature, remain invariant (see Appendix D).

Near the event horizon, the coupling $u(x)$ can be approximated by a linear profile

$$u(x) \approx 2\kappa(x - x_h), \quad (26)$$

where $\kappa = \frac{1}{2}u'(x_h)$ is the surface gravity associated with the Schwarzschild metric. This expression for κ can be obtained by mapping the Schwarzschild line element of Eq. (25) to a coordinate system that is regular at the horizon and applying the procedure described in Appendix B.1. In this near-horizon regime, the Schwarzschild metric reduces to the Rindler metric, which describes the space-time of a uniformly accelerating observer in Minkowski space with a constant proper acceleration κ (see Appendix B.2).

According to the Fulling-Davies-Unruh effect [61–63], such an observer perceives the Minkowski vacuum as a thermal state with temperature $T_H = \kappa/2\pi$ [4] (see Appendices B). It follows that the partitioned ground state of the mean-field Hamiltonian of Eq. (2), with the linear coupling $u(x)$ of Eq. (26) and $v = 0$, will be thermal with an effective temperature equal to the Hawking temperature T_H , as it approximates both the entanglement Hamiltonian and the Hamiltonian of a Dirac spinor in Rindler space-time [57, 59].

As in the Gullstrand-Painlevé case, the thermality of the Hamiltonian corresponding to a Dirac spinor in

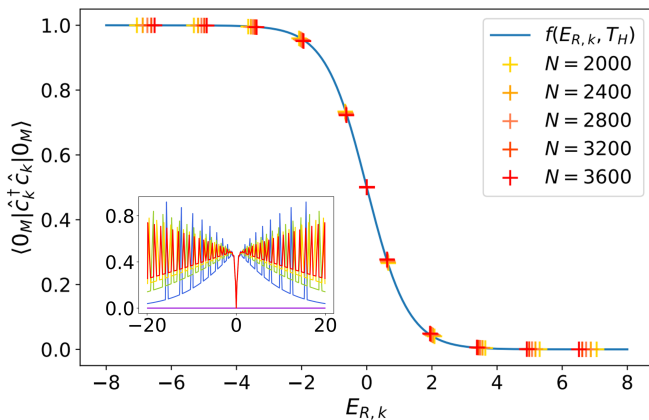


Figure 7. Data points show the mode occupation expectation values $\langle 0_M | c_k^\dagger c_k | 0_M \rangle$ of the mean-field Hamiltonian that simulates Rindler space-time (Eq. (2) with couplings $u(x) = \alpha(x/x_h - 1)$ and $v = 0$, defined only on \mathcal{B}), computed with respect to the Minkowski ground state $|0_M\rangle$ (Eq. (1) with $u = 1$ and $v = 0$, defined over the entire lattice). The abscissa shows the energy eigenvalues $E_{R,k}$ of the single-particle Hamiltonian h_R corresponding to H_{MF} with the Rindler couplings. The blue curves correspond to a Fermi-Dirac distribution with temperature $T_H = \kappa/2\pi$, where $\kappa = u'(x_h)/2 = \alpha/2x_h$ is the surface gravity associated with the linear coupling profile. System sizes $N = 2000, 2400, 2800, 3000$, and 3600 were considered, with the horizon located at $n_h = N/2$ and coupling slope $\alpha = 2$. Inset depicts the absolute interpolation error $|e(E_{R,k})|$ between numerical and interpolated data of the mode occupation for $\Delta n = 0, 20, 40, 60, 80$ (colour scheme as in Fig. 6a) with $N = 2000$ and $\alpha = 1/2$.

Rindler space-time can be confirmed by analysing the mode occupation of the partitioned system's ground state. Specifically, we compute the expectation value of the mode occupation operators with respect to the ground state $|0_M\rangle$ of the Minkowski Hamiltonian. As shown in Fig. 7, the resulting mode occupations for the Rindler Hamiltonian follow a Fermi-Dirac distribution with temperature $T_H = \kappa/2\pi$, thereby confirming the thermal nature of the reduced state and validating the extraction of the Hawking temperature via this approach. Once again, this thermality is only present when the lattice system is partitioned at the horizon.

VI. Discussion

We studied the mean-field theory limit of a chiral spin-chain simulator that, in its continuum limit, due to the emergence of an effective Lorentz invariance at low energies, describes a theory of Dirac fermions on a black hole space-time. For this model, we obtained analytic expressions for the fermion zero-mode entropy of the black hole space-time's interior and exterior regions. This entropy, derived under the assumption that the fermions are suitably described by a thermal Gibbs state with respect to any space-time bipartition, is finite as a result

of the spin-chain's non-linear dispersion relation, which naturally breaks the effective Lorentz invariance at the length scales of the lattice spacing.

By employing numerical simulations to investigate the spin-chain's entanglement entropy and comparing it with our analytic black hole fermion zero-mode entropy, we identified regimes where the two entropies are equivalent and, by extension, where the assumption of thermality is valid and where it breaks down. Mainly, we demonstrated that, with respect to an arbitrary partition, the thermality condition is generally not valid. This is due to the absence of interactions, as the mean-field system cannot truly thermalise. Instead, somewhat surprisingly, the thermality condition holds only when the partition is located at the event horizon, due to the unique physics emerging in that region. We further verified this by studying the mode occupation of the partitioned system, which revealed a thermal Fermi-Dirac distribution only for partitions near the event horizon.

When the chiral operator's coupling $v(x)$ is present, the mean-field Hamiltonian, which corresponds to that of a Dirac spinor on a Gullstrand-Painlevé space-time in its continuum limit, does not approximate an entanglement Hamiltonian. Hence, the temperature of this thermal distribution does not agree with the Hawking temperature. To extract the Hawking temperature, $v(x)$ must be set to zero, and the curvature needs to be encoded in a linear coupling $u(x)$ of the nearest-neighbour tunnellings. In the continuum limit, taking these couplings is equivalent to performing a coordinate transformation from Gullstrand-Painlevé to Rindler space-time, which approximates Schwarzschild space-time near the black hole's horizon. In this case, the mean-field Hamiltonian approximates both the entanglement Hamiltonian and the Hamiltonian of a Dirac spinor in Rindler space-time; thus, the Hawking temperature can be extracted from the mode occupation's thermal distribution. Once again, this thermal distribution breaks down as the partition deviates from the event horizon.

The breakdown of thermality for arbitrary partitions indicates that no genuine thermalisation occurs in the free-theory regime, implying that the simulated black hole's information is not entirely erased. Beyond the mean-field limit, we expect strong interactions inside the simulated black hole to induce genuine thermalisation, resulting in a thermal distribution even for sufficiently small, but otherwise arbitrary partitions. Further investigation of thermalisation in this strong interaction regime is a potential avenue for future research, along with generalising the chiral spin-chain to higher-dimensional systems and exploring the interplay between Hamiltonian perturbations and coordinate transformation in the continuum limit.

Acknowledgements

We are grateful to Cristian Voinea, Matthew Horner, Aiden Daniel, and Tanmay Bhore for their insightful discussions and guidance. This work was supported by EPSRC with Grant Nos. EP/W524372/1 and

UKRI1337:Anyons24. Statement of compliance with EPSRC policy framework on research data: This publication is theoretical work that does not require supporting research data. A.H. acknowledges support from Leverhulme Trust Research Leadership Award RL-2019-015.

-
- [1] J. M. Bardeen, B. Carter, and S. W. Hawking, The four laws of black hole mechanics, *Commun. Math. Phys.* **31**, 161 (1973).
- [2] J. D. Bekenstein, Black holes and entropy, *Phys. Rev. D* **7**, 2333 (1973).
- [3] J. D. Bekenstein, Generalized second law of thermodynamics in black-hole physics, *Phys. Rev. D* **9**, 3292 (1974).
- [4] R. M. Wald, *Quantum Field Theory in Curved Spacetime and Black Hole Thermodynamics* (University of Chicago Press, 1994).
- [5] S. W. Hawking, Gravitational radiation from colliding black holes, *Phys. Rev. Lett.* **26**, 1344 (1971).
- [6] S. W. Hawking, Particle creation by black holes, *Communications in Mathematical Physics* **43**, 199 (1975).
- [7] S. W. Hawking, Breakdown of predictability in gravitational collapse, *Phys. Rev. D* **14**, 2460 (1976).
- [8] S. A. and V. C., Microscopic origin of the bekenstein-hawking entropy, *Physics Letters B* **379**, 99 (1996).
- [9] T. Jacobson, *Black hole entropy and induced gravity* (1994), [arXiv:gr-qc/9404039](https://arxiv.org/abs/gr-qc/9404039) [gr-qc].
- [10] L. Susskind and J. Uglum, Black hole entropy in canonical quantum gravity and superstring theory, *Phys. Rev. D* **50**, 2700 (1994).
- [11] A. D. Sakharov, Vacuum quantum fluctuations in curved space and the theory of gravitation, *Soviet Physics Uspekhi* **34**, 394 (1967).
- [12] R. M. Wald, On particle creation by black holes, *Communications in Mathematical Physics* **45**, 9 (1975).
- [13] R. M. Wald, The thermodynamics of black holes, *Living Reviews in Relativity* **4**, 10.12942/lrr-2001-6 (2001).
- [14] T. G. Philbin, C. Kuklewicz, S. Robertson, S. Hill, F. König, and U. Leonhardt, Fiber-optical analog of the event horizon, *Science* **319**, 1367 (2008).
- [15] S. Weinfurter, E. W. Tedford, M. C. J. Penrice, W. G. Unruh, and G. A. Lawrence, Measurement of stimulated hawking emission in an analogue system, *Physical Review Letters* **106**, 10.1103/physrevlett.106.021302 (2011).
- [16] H. S. Nguyen, G. Dario, I. Carusotto, D. Sanvitto, E. Galopin, A. Lemaître, I. Sagnes, J. Bloch, and A. Amo, Acoustic black hole in a stationary hydrodynamic flow of microcavity polaritons, *Physical Review Letters* **114**, 10.1103/physrevlett.114.036402 (2015).
- [17] J. R. Muñoz de Nova, K. Golubkov, V. I. Kolobov, and J. Steinhauer, Observation of thermal hawking radiation and its temperature in an analogue black hole, *Nature* **569**, 688–691 (2019).
- [18] V. I. Kolobov, K. Golubkov, J. R. Muñoz de Nova, and J. Steinhauer, Observation of stationary spontaneous hawking radiation and the time evolution of an analogue black hole, *Nature Physics* **17**, 10.1038/s41567-020-01076-0 (2021).
- [19] J. Hu, L. Feng, Z. Zhang, and C. Chin, Quantum simulation of unruh radiation, *Nature Physics* **15**, 785 (2019).
- [20] Y.-H. Shi, R.-Q. Yang, Z. Xiang, Z.-Y. Ge, H. Li, Y.-Y. Wang, K. Huang, Y. Tian, X. Song, D. Zheng, K. Xu, R.-G. Cai, and H. Fan, Quantum simulation of hawking radiation and curved spacetime with a superconducting on-chip black hole, *Nature Communications* **14**, 3263 (2023).
- [21] B. Rhyno, B. Lapierre, S. Vishveshwara, K. Najafi, and R. Chitra, *Observing quantum many-body dynamics in emergent curved spacetime using programmable quantum processors* (2026), [arXiv:2602.15524](https://arxiv.org/abs/2602.15524) [quant-ph].
- [22] W. G. Unruh, Experimental black-hole evaporation?, *Phys. Rev. Lett.* **46**, 1351 (1981).
- [23] W. G. Unruh, Sonic analogue of black holes and the effects of high frequencies on black hole evaporation, *Phys. Rev. D* **51**, 2827 (1995).
- [24] C. Barceló, S. Liberati, and M. Visser, Analogue gravity, *Living Reviews in Relativity* **8**, 10.12942/lrr-2005-12 (2005).
- [25] G. E. Volovik, Superfluid analogies of cosmological phenomena, *Physics Reports* **351**, 195 (2001).
- [26] G. E. Volovik, *The Universe in a Helium Droplet*, 2nd ed. (Clarendon Press, 2003).
- [27] G. E. Volovik, Fermion zero modes in painlevé-gullstrand black hole, *Journal of Experimental and Theoretical Physics Letters* **73**, 637–641 (2001).
- [28] P. Huhtala and G. E. Volovik, Fermionic microstates within the painlevé-gullstrand black hole, *Journal of Experimental and Theoretical Physics* **94**, 853– (2002).
- [29] M. D. Horner, *Emergent Spacetime in Quantum Lattice Models*, *Thesis*, University of Leeds (2022).
- [30] M. D. Horner, A. Hallam, and J. K. Pachos, Chiral spin-chain interfaces exhibiting event-horizon physics, *Phys. Rev. Lett.* **130**, 016701 (2023).
- [31] E. Forbes, M. D. Horner, A. Hallam, J. Barker, and J. K. Pachos, Exploring interacting chiral spin chains in terms of black hole physics, *Phys. Rev. B* **108**, 245142 (2023).
- [32] A. Daniel, A. Hallam, M. D. Horner, and J. K. Pachos, *Optimally scrambling chiral spin-chain with effective black hole geometry* (2024), [arXiv:2404.14473](https://arxiv.org/abs/2404.14473) [cond-mat.str-el].
- [33] S. Corley and T. Jacobson, Hawking spectrum and high frequency dispersion, *Phys. Rev. D* **54**, 1568 (1996).
- [34] S. Corley and T. Jacobson, Lattice black holes, *Phys. Rev. D* **57**, 6269 (1998).
- [35] S. Corley, Computing the spectrum of black hole radiation in the presence of high frequency dispersion: An analytical approach, *Phys. Rev. D* **57**, 6280 (1998).
- [36] S. Corley and T. Jacobson, Black hole lasers, *Phys. Rev. D* **59**, 124011 (1999).
- [37] T. Jacobson and R. Parentani, Black hole entanglement entropy regularized in a freely falling frame, *Phys. Rev.*

- D **76**, 024006 (2007).
- [38] C. Holzhey, F. Larsen, and F. Wilczek, Geometric and renormalized entropy in conformal field theory, *Nuclear Physics B* **424**, 443 (1994).
- [39] G. Vidal, J. I. Latorre, E. Rico, and A. Kitaev, Entanglement in quantum critical phenomena, *Phys. Rev. Lett.* **90**, 227902 (2003).
- [40] P. Calabrese and J. Cardy, Entanglement entropy and quantum field theory, *Journal of Statistical Mechanics: Theory and Experiment* **2004**, P06002 (2004).
- [41] S. Mukohyama, *Aspects of black hole entropy* (1999), [arXiv:gr-qc/9912103 \[gr-qc\]](https://arxiv.org/abs/gr-qc/9912103).
- [42] S. M. Chandran and S. Shankaranarayanan, One-to-one correspondence between entanglement mechanics and black hole thermodynamics, *Phys. Rev. D* **102**, 125025 (2020).
- [43] A. Belfiglio, S. M. Chandran, O. Luongo, and S. Mancini, Horizon entanglement area law from regular black hole thermodynamics, *Phys. Rev. D* **111**, 024013 (2025).
- [44] P. Hayden and J. Preskill, Black holes as mirrors: quantum information in random subsystems, *Journal of High Energy Physics* **2007**, 120 (2007).
- [45] C. D’Cruz and J. K. Pachos, Chiral phase from three-spin interactions in an optical lattice, *Phys. Rev. A* **72**, 043608 (2005).
- [46] D. I. Tsomokos, J. J. García-Ripoll, N. R. Cooper, and J. K. Pachos, Chiral entanglement in triangular lattice models, *Phys. Rev. A* **77**, 012106 (2008).
- [47] A. Gullstrand, Allgemeine lösung des statischen einkörperproblems in der einsteinschen gravitationstheorie, *Ark. Mat. Astr. Fys.* **16**, 1 (1922).
- [48] P. Painlevé, La mécanique classique et la théorie de la relativité, *C. R. Acad. Sci. (Paris)* **173**, 677 (1921).
- [49] A. Daniel, T. Bhore, J. K. Pachos, C. Liu, and A. Hallam, [Quantum teleportation between simulated binary black holes](https://arxiv.org/abs/2503.10761) (2025), [arXiv:2503.10761 \[cond-mat.str-el\]](https://arxiv.org/abs/2503.10761).
- [50] M. K. Parikh and F. Wilczek, Hawking radiation as tunneling, *Phys. Rev. Lett.* **85**, 5042 (2000).
- [51] L. Bombelli, R. K. Koul, J. Lee, and R. D. Sorkin, Quantum source of entropy for black holes, *Phys. Rev. D* **34**, 373 (1986).
- [52] C. Callan and W. F., On geometric entropy, *Physics Letters B* **333**, 55 (1994).
- [53] M. Robert, The dilogarithm function of a real argument, *Mathematics of Computation* **33**, 778 (1979).
- [54] L. Lewin and J. C. P. Miller, *Dilogarithms and associated functions; 1st publ.* (Macdonald, London, 1958) p. 353 p.
- [55] I. Peschel, Calculation of reduced density matrices from correlation functions, *Journal of Physics A: Mathematical and General* **36**, L205 (2003).
- [56] I. Klich, Lower entropy bounds and particle number fluctuations in a fermi sea, *Journal of Physics A: Mathematical and General* **39**, L85 (2006).
- [57] L. Mertens, A. G. Moghaddam, D. Chernyavsky, C. Morice, J. van den Brink, and J. van Wezel, Thermalization by a synthetic horizon, *Phys. Rev. Res.* **4**, 043084 (2022).
- [58] I. Peschel and V. Eisler, Reduced density matrices and entanglement entropy in free lattice models, *Journal of Physics A: Mathematical and Theoretical* **42**, 504003 (2009).
- [59] A. Deger, M. D. Horner, and J. K. Pachos, Ads/cft correspondence with a three-dimensional black hole simulator, *Phys. Rev. B* **108**, 155124 (2023).
- [60] R.-Q. Yang, H. Liu, S. Zhu, L. Luo, and R.-G. Cai, Simulating quantum field theory in curved spacetime with quantum many-body systems, *Phys. Rev. Res.* **2**, 023107 (2020).
- [61] S. A. Fulling, Nonuniqueness of canonical field quantization in riemannian space-time, *Phys. Rev. D* **7**, 2850 (1973).
- [62] P. C. W. Davies, Scalar production in schwarzschild and rindler metrics, *Journal of Physics A: Mathematical and General* **8**, 609 (1975).
- [63] W. G. Unruh, Notes on black-hole evaporation, *Phys. Rev. D* **14**, 870 (1976).
- [64] S. Weinberg, *Gravitation and Cosmology: Principles and Applications of the General Theory of Relativity* (John Wiley and Sons, New York, 1972).
- [65] L. Parker and D. Toms, *Quantum Field Theory in Curved Spacetime: Quantized Fields and Gravity*, Cambridge Monographs on Mathematical Physics (Cambridge University Press, 2009).
- [66] S. M. Carroll, *Spacetime and Geometry: An Introduction to General Relativity* (Cambridge University Press, 2019).
- [67] A. Farjami, M. D. Horner, C. N. Self, Z. Papić, and J. K. Pachos, Geometric description of the kitaev honeycomb lattice model, *Phys. Rev. B* **101**, 245116 (2020).
- [68] M. Nakahara, *Geometry, Topology and Physics*, 2nd ed. (Taylor and Francis, 2003).
- [69] R. M. Wald, *General relativity* (University of Chicago Press, 1984).
- [70] W. Rindler, *Special relativity.*, 2nd ed., University mathematical texts (Oliver & Boyd, Edinburgh, 1966).
- [71] W. Rindler, *Essential relativity : special, general, and cosmological*, revised second ed., Texts and monographs in physics (Springer, New York, 1977).
- [72] S. A. Fulling, *Scalar Quantum Field Theory in a Closed Universe of Constant Curvature*, [Thesis](https://arxiv.org/abs/1907.08561) (1972).
- [73] S. A. Fulling, *Aspects of Quantum Field Theory in Curved Spacetime*, London Mathematical Society Student Texts (Cambridge University Press, 1989).

Appendix A. Spinor fields on a (1+1)D Riemann-Cartan space-time

This appendix is devoted to introducing the vielbein formalism of general relativity, which is the mathematical formalism required for dealing with spinors on a curved space-time. This formalism is required as the standard method for transitioning from special to general relativity, in which the Minkowski metric tensor $\eta_{\mu\nu}$ is replaced by the general covariant metric tensor $g_{\mu\nu}$ and partial derivatives ∂_μ (equivalently denoted $;\mu$) by covariant derivatives ∇_μ (equivalently denoted $;\mu$), works only for objects that transform as tensors under Lorentz transformations, not for spinors, which are the mathematical objects that describe fermions [64].

1 Vielbein Formalism

Consider an n -dimensional space-time M with local coordinates $\{x^\mu\}$, where $x^\mu \in \{t, x, y, z, \dots\}$ labels the coordinate axes, with coordinate basis vectors $\{e_\mu = \partial_\mu\}$ and dual basis vectors $\{e^\mu = dx^\mu\}$ that span the cotangent space of M , which satisfy $e^\mu e_\nu = \delta_\nu^\mu$ [65]. Greek indices $\mu, \nu, \dots \in \{t, x, y, z, \dots\}$ are used to denote components with respect to the coordinate basis $\{e_\mu\}$. In the coordinate basis, the line element ds^2 of the space-time M can be expressed as

$$ds^2 = g_{\mu\nu}(x)dx^\mu dx^\nu, \quad (\text{A.1})$$

where $g_{\mu\nu}$ is the covariant metric tensor of space-time M [65]. At any point p on the space-time, the Principle of Equivalence can be used to construct a set of coordinates, spanned by the orthonormal basis vectors $\{e_a\}$ with the corresponding dual basis vectors $\{e^a\}$, which are locally flat at p [64]. In such a coordinate system, the line element ds^2 is given by

$$ds^2 = \eta_{ab}e^a(x)e^b(x), \quad (\text{A.2})$$

where η_{ab} is the Minkowski metric tensor [65]. As both $\{e^\mu = dx^\mu\}$ and $\{e^a(x)\}$ span the cotangent space of M , it is possible to relate the two bases via

$$e^a(x) = e_\mu^a(x)dx^\mu, \quad (\text{A.3})$$

where the coefficients $e_\mu^a(x)$ are referred to as the vielbein (in two-, three- and four-dimensional space-times, these coefficients are often referred to as zweibein, dreibein and vierbein, respectively) [65]. Latin indices $a, b, \dots \in \{0, 1, 2, 3, \dots\}$ are used to denote components with respect to the vielbein basis $\{e_a\}$.

Substitution of Eq. (A.3) for the relation between the vielbein and coordinate bases into Eq. (A.2) for the line element as expressed in the vielbein basis, then comparing to Eq. (A.1) for the line element as expressed in the coordinate basis, yields [65]

$$g_{\mu\nu}(x) = \eta_{ab}e_\mu^a(x)e_\nu^b(x), \quad (\text{A.4})$$

which expresses the general covariant metric tensor in terms of the Minkowski metric and vielbein. The vielbein and their dual vectors, denoted $e_a^\mu(x)$, satisfy the relations [65]

$$e_a^\mu(x)e_\nu^a(x) = \delta_\nu^\mu, \quad e_\mu^a(x)e_b^\mu(x) = \delta_b^a, \quad (\text{A.5})$$

which, along with Eqs. (A.3) and (A.4) for the definition of the vielbein and the general covariant metric tensor in terms of the vielbein, respectively, can be used to obtain

$$g^{\mu\nu}(x) = \eta^{ab}e_a^\mu(x)e_b^\nu(x). \quad (\text{A.6})$$

For a vector \mathbf{X} , the vielbein and their duals can be used to relate the vector's components in each basis via $X^\mu = e_a^\mu X^a$ and $X^a = e_\mu^a X^\mu$. The general covariant and

contravariant metric tensors, $g_{\mu\nu}$ and $g^{\mu\nu}$, can be used to lower and raise coordinate indices, respectively. That is, $g_{\mu\nu}X^\nu = X_\mu$ and $g^{\mu\nu}X_\nu = X^\mu$. The covariant and contravariant Minkowski metric tensors, η_{ab} and η^{ab} , can be used to lower and raise vielbein indices, respectively. That is, $\eta_{ab}X^b = X_a$ and $\eta^{ab}X_b = X^a$ [64].

2 Torsion, spin connection and Riemann-Cartan space-time

To introduce a covariant derivative, which allows for the derivatives of tensors to be taken, a connection that describes how tensors should be transported around a space-time must be introduced. This enables tensors to be compared at infinitesimally separated points on the space-time, which allows the tensor's covariant derivative to be defined. The standard method for defining this connection is to impose that the lengths of, and angles between, a pair of vectors remain unchanged when being transported along a space-time [29]. This method of transporting vectors is known as parallel transport and requires that $d\mathbf{X}/d\lambda = 0$, where λ is some affine parameter.

The choice of connection defines the covariant derivative of a tensor. For example, the covariant derivative of a rank (1, 1) tensor A_ν^μ , expressed in terms of the coordinate basis, is given by

$$\nabla_\alpha A_\nu^\mu = \partial_\alpha A_\nu^\mu + \Gamma_{\alpha\beta}^\mu A_\nu^\beta - \Gamma_{\alpha\nu}^\beta A_\beta^\mu, \quad (\text{A.7})$$

where $\Gamma_{\beta\gamma}^\alpha$ are the components of the connection. In standard general relativity, the connection that is chosen is the Levi-Civita connection $\Gamma_{\beta\gamma}^\alpha = \tilde{\Gamma}_{\beta\gamma}^\alpha$, which is completely determined by the metric and is given by [66]

$$\tilde{\Gamma}_{\beta\gamma}^\alpha = \frac{1}{2}g^{\alpha\mu}(\partial_\gamma g_{\beta\mu} + \partial_\beta g_{\gamma\mu} - \partial_\mu g_{\beta\gamma}). \quad (\text{A.8})$$

The connection coefficients $\tilde{\Gamma}_{\beta\gamma}^\alpha$ are often also referred to as the Christoffel symbols. The connection that is chosen for spinors is called the spin connection $\omega_{\mu b}^a$ and, in the vielbein basis, is given by [67]

$$\omega_{\mu b}^a = e_a^\alpha \nabla_\mu e_b^\alpha = e_a^\alpha \left(\partial_\mu e_b^\alpha + \Gamma_{\mu\beta}^\alpha e_b^\beta \right), \quad (\text{A.9})$$

as it allows for the action that a covariant derivative has on a vielbein basis vector to be defined as $\nabla_\mu e_a = \omega_{\mu a}^b e_b$ [29]. Space-times with the spin connection are known as Riemann-Cartan space-times. The *dreibein postulate* states that the covariant derivative of the dual dreibein e_a^ν is zero. That is, $\nabla_\mu e_a^\nu = 0$ [67]. For this spin connection, the covariant derivative of a rank (1, 1) tensor A_b^a in the vielbein basis is given by [67]

$$\nabla_\mu A_b^a = \partial_\mu A_b^a + \omega_{\mu c}^a A_b^c - \omega_{\mu b}^c A_c^a. \quad (\text{A.10})$$

3 Spinor field on a Riemann-Cartan space-time

The action for a Dirac spinor ψ of mass m on a general (1+1)-dimensional Riemann-Cartan space-time M is given by [68]

$$S_{RC} = \int_M d^{1+1}x \mathcal{L}_{RC}, \quad (\text{A.11})$$

$$= \frac{i}{2} \int_M d^{1+1}x |e| (\bar{\psi} \gamma^\mu D_\mu \psi - \overline{D_\mu \psi} \gamma^\mu \psi + 2im \bar{\psi} \psi), \quad (\text{A.12})$$

where \mathcal{L}_{RC} is the Lagrangian density, γ^μ denotes the curved space-time gamma matrices that obey the anti-commutation relations $\{\gamma^\mu, \gamma^\nu\} = 2g^{\mu\nu}$ and are related to the flat space-time gamma matrices γ^a via $\gamma^\mu = e_a^\mu \gamma^a$, which themselves obey the anti-commutation relations $\{\gamma^a, \gamma^b\} = 2\eta^{ab}$. The flat space-time gamma matrix γ^0 allows the Dirac adjoint $\bar{\psi} = \psi^\dagger \gamma^0$ to be defined. Here, D_μ denotes the covariant derivative of the spinor ψ and $\overline{D_\mu \psi}$ denotes their adjoint, both of which are given by [67]

$$D_\mu \psi = \partial_\mu \psi + \omega_\mu \psi, \quad (\text{A.13})$$

$$\overline{D_\mu \psi} = (D_\mu \psi)^\dagger \gamma^0 = \partial_\mu \bar{\psi} - \bar{\psi} \omega_\mu, \quad (\text{A.14})$$

respectively, where ω_μ is given by [67]

$$\omega_\mu = \frac{i}{2} \omega_{\mu ab} \Sigma^{ab}, \quad \Sigma^{ab} = \frac{i}{4} [\gamma^a, \gamma^b], \quad (\text{A.15})$$

and $\omega_{\mu ab} = \eta_{ac} \omega_{\mu b}^c$. The notations D_μ and ∇_μ are used to distinguish between the covariant derivative acting on spinors and tensors, respectively.

From Eqs. (A.13) and (A.14) for the spinor covariant derivative and its adjoint, and the fact that $\{\omega_\mu, \gamma^\mu\} \propto \{\gamma^a, [\gamma^b, \gamma^c]\} = 0$ in (1+1)-dimensions, Eq. (A.12) for the action of a massive Dirac spinor on a (1+1)-dimensional Riemann-Cartan space-time can be expressed as

$$S_{RC} = i \int_M d^{1+1}x |e| \left(\bar{\psi} \gamma^\mu \overleftrightarrow{\partial}_\mu \psi + im \bar{\psi} \psi \right). \quad (\text{A.16})$$

The canonical momentum $\pi(t, x)$ conjugate to $\psi(t, x)$ is defined as

$$\pi(t, x) = \frac{\partial \mathcal{L}}{\partial(\partial_t \psi)}, \quad (\text{A.17})$$

which, for a Dirac spinor on a general Riemann-Cartan space-time, is given by

$$\pi(t, x) = \frac{i}{2} |e| \psi^\dagger(t, x) \gamma^0 \gamma^t. \quad (\text{A.18})$$

To quantise the action for the Dirac spinor on a general Riemann-Cartan space-time given in Eq. (A.12), $\psi(t, x)$ and $\pi(t, x)$ are promoted to Hermitian operators $\hat{\psi}(t, x)$

and $\hat{\pi}(t, x)$ and are required to satisfy the following equal-time canonical anti-commutation relations [65]:

$$\begin{aligned} \{\hat{\psi}_\alpha(t, x), \hat{\psi}_\beta(t, x')\} &= \{\hat{\pi}_\alpha(t, x), \hat{\pi}_\beta(t, x')\} = 0, \\ \{\hat{\psi}_\alpha(t, x), \hat{\pi}_\beta(t, x')\} &= i \delta_{\alpha\beta} \delta(x - x'), \end{aligned} \quad (\text{A.19})$$

where α, β denote spinor components. Using these canonical anti-commutation relations and Eq. (A.18) for the canonical momentum of a Dirac spinor, one obtains the following additional anti-commutation relation between the field operator $\hat{\psi}$ and its Hermitian conjugate $\hat{\psi}^\dagger$:

$$\{\hat{\psi}_\alpha(t, x), \hat{\psi}_\beta^\dagger(t, x')\} = \frac{1}{|e|} (\gamma^0 \gamma^t)^{-1} \delta_{\alpha\beta} \delta(x - x'). \quad (\text{A.20})$$

If the space-time M is described by a stationary metric (that is, a metric that is invariant under the time-translation transformation $t \mapsto t + t_0$, where $t_0 \in \mathbb{R}$), then it will admit a time-like Killing vector $\xi^\mu = \delta_t^\mu$ (often equivalently denoted ∂_t) satisfying the Killing equation of Eq (B.1). Consequently, the energy of the spinor will be a well-defined quantity that is conserved along the metric's geodesics [28, 65]. This allows a Hamiltonian H to be defined via the following Legendre transformation of the Lagrangian density: [67]

$$H = \int_S dx \left(\frac{\partial \mathcal{L}}{\partial(\partial_t \psi)} \partial_t \psi - \mathcal{L} \right), \quad (\text{A.21})$$

Computing this Legendre transformation for the Lagrangian density of a spinor field in a (1+1)-dimensional Riemann-Cartan space-time yields the following Hamiltonian for a spinor on a Riemann-Cartan space-time: [65]

$$\hat{H} = \int_S dx \left(\hat{\pi} \partial_t \hat{\psi} \right). \quad (\text{A.22})$$

Appendix B. Hawking effect in chiral black hole metric

In this appendix, the Hawking effect is derived for a (1+1)-dimensional Schwarzschild black hole. The method of this derivation follows that of Refs. [57, 59], which utilises the equivalence between the Hawking effect and the Fulling-Davies-Unruh effect near the event horizon of a black hole. This equivalence is due to the fact that, near the event horizon, the Schwarzschild metric can be approximated by the Rindler metric, which describes a uniformly accelerating observer. This technique is used as it is more straightforward to analytically solve the Dirac equation and construct a quantum field theory in a space-time described by the Rindler metric than in a space-time described by the Schwarzschild or Gullstrand-Painlevé metrics. For brevity, the detailed mathematical construction of this quantum field theory in Rindler space-time is omitted, and the emphasis is instead on presenting the fundamental building blocks of

this derivation. The final result of this section will be that an observer near the event horizon of the black hole will experience the Fulling-Davies-Unruh effect [61–63] with a temperature equal to the Hawking temperature of the black hole.

1 Surface gravity of Gullstrand-Painlevé metric

Consider the (1+1)-dimensional Gullstrand-Painlevé metric line element given in Eq. (10), which is the line element of the (1+1)-dimensional Schwarzschild metric expressed in Gullstrand-Painlevé coordinates $x^\mu = (t, x)$. Here, the couplings u and v are independent of t , but not necessarily of x ; thus, the metric is stationary, though not static [26]. As the Gullstrand-Painlevé metric is stationary, it admits a Killing vector $\xi^\mu = \delta_t^\mu = (1, 0)$ [65], which is time-like in the region $u^2 > v^2$ and satisfies the Killing equation

$$\xi_{\mu;\nu} + \xi_{\nu;\mu} = 0. \quad (\text{B.1})$$

The vector $\xi_\mu = g_{\mu\nu}\xi^\nu = (1 - v^2/u^2, -v/u^2)$ is also a Killing vector that satisfies the Killing equation. As the Gullstrand-Painlevé metric is regular at the event horizon x_h , these Killing vectors can be used to find the surface gravity κ of the black hole space-time, as defined by a distant observer, by evaluating

$$\xi^\mu \xi_{\nu;\mu} = \xi^\mu \left(\xi_{\nu,\mu} - \xi_\gamma \tilde{\Gamma}_{\nu\mu}^\gamma \right) = \kappa \xi_\nu, \quad (\text{B.2})$$

at the black hole's event horizon [4, 69].

Expanding the Einstein summations over μ and γ , and making use of the fact that $\xi_{\nu,t} = \nabla_\nu$, $\xi^t = 1$, and $\xi^x = 0$, Eq. (B.2) for the surface gravity can be expressed as

$$-\xi_x \tilde{\Gamma}_{\nu t}^x - \xi_t \tilde{\Gamma}_{\nu t}^t = \kappa \xi_\nu, \quad (\text{B.3})$$

which, using the only relevant and non-zero Christoffel coefficients $\tilde{\Gamma}_{xt}^t = \frac{1}{2}g^{tt}g_{tt,x}$ and $\tilde{\Gamma}_{xt}^x = \frac{1}{2}g^{xt}g_{tt,x}$, can be solved for $\nu = x$ to yield

$$-\frac{1}{2}\xi_t g^{tt}g_{tt,x} - \frac{1}{2}\xi_x g^{xt}g_{tt,x} = \kappa \xi_x. \quad (\text{B.4})$$

Substitution of the relevant values for the components of the metric tensor corresponding to the Gullstrand-Painlevé line element of Eq. (10) into the above equation and evaluating the resultant expression at the event horizon gives the following surface gravity:

$$\kappa = \pm \frac{du(x_h)}{dx} - \frac{dv(x_h)}{dx}. \quad (\text{B.5})$$

2 Dirac equation in Rindler space-time

Henceforth, we take v to be a slowly varying position-dependent function $v(x)$ and restrict ourselves to the case

where $u = 1$, such that the Gullstrand-Painlevé line element of Eq. (10) simplifies to

$$ds^2 = (1 - v(x)^2) dt^2 - 2v(x) dt dx - dx^2, \quad (\text{B.6})$$

where $v(x)$ satisfies $v(x_h) = \pm 1$, and $v(x) \rightarrow 0$ as $x \rightarrow \infty$ such that the metric of Eq. (B.6) is *asymptotically flat*. The coordinate transformation $(t, x) \mapsto (\tilde{t}, x)$ between Gullstrand-Painlevé coordinates $x^\mu = (t, x)$ and Schwarzschild coordinates $\tilde{x}^\mu = (\tilde{t}, x)$, where

$$t(\tilde{t}, x) = \tilde{t} + \int dx \frac{v(x)}{1 - v(x)^2}, \quad (\text{B.7})$$

can be used to map the Gullstrand-Painlevé metric line element of Eq. (B.6) to

$$ds^2 = (1 - v(x)^2) d\tilde{t}^2 - \frac{dx^2}{1 - v(x)^2}, \quad (\text{B.8})$$

which is equivalent to the (1+1)-dimensional Schwarzschild metric when $v(x) = \sqrt{x_h/x}$. The metric of Eq. (B.8) contains a coordinate singularity at $v(x_h) = \pm 1$ and is therefore only valid in the region $x > x_h$ that describes the black hole's exterior.

The function $f(x) = 1 - v(x)^2$ can be Taylor expanded about x_h as

$$f(x) \simeq 2\kappa(x - x_h) + O(x^2), \quad (\text{B.9})$$

where the metric's surface gravity $\kappa = -v'(x_h)$ has been identified. Hence, near the event horizon of the black hole, Eq. (B.8) for the Schwarzschild metric line element can be expressed as

$$ds^2 = 2\kappa(x - x_h) d\tilde{t}^2 - \frac{dx^2}{2\kappa(x - x_h)}. \quad (\text{B.10})$$

A further coordinate transformation $(\tilde{t}, x) \mapsto (\tilde{t}, \rho)$, where

$$\rho^2 = \frac{2(x - x_h)}{\kappa}, \quad (\text{B.11})$$

can be employed to map Eq. (B.10) for the line element of the Schwarzschild metric near the horizon to

$$ds^2 = (\kappa\rho)^2 d\tilde{t}^2 - d\rho^2, \quad (\text{B.12})$$

which is the Rindler metric line element [70, 71] that describes an observer that is uniformly accelerating in Minkowski space-time with a constant proper acceleration κ . The coordinates $x_R^\mu = (\tilde{t}, \rho)$ will be referred to as Rindler coordinates. The Rindler metric possesses a coordinate singularity at $\rho = 0$, which corresponds to the coordinate singularity at x_h of the Schwarzschild metric. For this reason, we leave the Rindler metric undefined for the region $\rho < 0$ [57]. The zweibein corresponding to the Rindler metric line element of Eq. (B.12) is given by $e_\mu^a = \text{diag}(\kappa\rho, 1)$.

We now proceed with solving the Dirac equation for a spinor $\psi(\tilde{t}, \rho)$ in a space-time described by the Rindler metric. The Dirac equation for a massive spinor ψ on a general Riemann-Cartan space-time reads

$$(i\gamma^\mu D_\mu - m)\psi = 0, \quad (\text{B.13})$$

$$\frac{i}{2}\gamma^\mu \partial_\mu \psi + \frac{i}{2} \frac{1}{|e|} \partial_\mu (|e| \gamma^\mu \psi) - \frac{i}{2} \{\gamma^\mu, \omega_\mu\} \psi - m\psi = 0, \quad (\text{B.14})$$

which in (1+1)-dimensions simplifies to

$$\frac{i}{2}\gamma^a e_a^\mu \partial_\mu \psi + \frac{i}{2} \frac{1}{|e|} \gamma^a \partial_\mu (|e| e_a^\mu \psi) - m\psi = 0 \quad (\text{B.15})$$

due to the fact that $\{\gamma^\mu, \omega_\mu\} \propto \{\gamma^a, [\gamma^b, \gamma^c]\} = 0$. As the Rindler metric is stationary with respect to the Rindler time coordinate \tilde{t} , it admits a Killing vector $\zeta^\mu = \delta_{\tilde{t}}^\mu$ (or equivalently $\partial_{\tilde{t}}$) that is time-like in the region $\rho > 0$. Hence, the energy $\epsilon = p_{\tilde{t}}$ of the spinor is a well-defined quantity that is conserved along the Rindler metric's geodesics [28, 65]. Therefore, the Dirac equation can be solved via the separation of variables [28, 61, 72]

$$\psi(\tilde{t}, \rho) = e^{-i\epsilon_k \tilde{t}} \psi_{\epsilon_k}(\rho). \quad (\text{B.16})$$

Substitution of this solution, along with the components of the Rindler metric zweibein, into the Dirac equation of Eq. (B.15) yields the following eigenvalue equation

$$h_R \psi_{\epsilon_k}(\rho) = \epsilon_k \psi_{\epsilon_k}(\rho), \quad (\text{B.17})$$

where

$$h_R = i\kappa \rho \gamma^0 \gamma^1 \partial_\rho + \frac{i}{2} \kappa \gamma^0 \gamma^1 - m \kappa \rho \gamma^0 \quad (\text{B.18})$$

is a linear differential operator that is Hermitian under the conserved inner product

$$\langle \phi(\rho), \psi(\rho) \rangle = \int d\mu(\rho) \phi(\rho)^\dagger \psi(\rho), \quad (\text{B.19})$$

and $d\mu(\rho) = d\rho$ is a measure of integration. That is, h_R is Hermitian as it satisfies $\langle \phi, h_R \psi \rangle = \langle h_R \phi, \psi \rangle$ [73]. Restricting ourselves to the case of a massless spinor and choosing the chiral representation of the γ matrices, $\gamma^0 = i\sigma^x$ and $\gamma^1 = \sigma^y$, the Hermitian operator h_R can be expressed as

$$h_R = -i\kappa \rho \sigma^z \partial_\rho - \frac{i}{2} \kappa \sigma^z. \quad (\text{B.20})$$

This allows the eigenvalue equation given in Eq. (B.17) to be expressed as the two following decoupled differential equations:

$$\epsilon_k \psi_{\epsilon_k}^\pm(\rho) \pm i\kappa \rho \partial_\rho \psi_{\epsilon_k}^\pm(\rho) \pm \frac{i\kappa}{2} \psi_{\epsilon_k}^\pm(\rho) = 0, \quad (\text{B.21})$$

where $\psi_{\epsilon_k}^\pm(\rho)$ denote the components of the spinor $\psi_{\epsilon_k}(\rho)$ that have solutions $\psi_{\epsilon_k}^\pm(\rho) = \mathcal{N} \rho^{\pm \frac{i\epsilon_k}{\kappa} - \frac{1}{2}}$ [57, 59]. Here,

\mathcal{N} is a normalisation constant that is chosen such that $\langle \psi_{\epsilon_k}, \psi_{\epsilon_q} \rangle = \delta(k - q)$, which, using the Dirac delta identity $\int_0^\infty x^{i\alpha-1} dx = 2\pi \delta(\alpha)$, can be determined to be $\mathcal{N} = 1/\sqrt{2\pi|\kappa|}$ [57]. Thus, as a solution $\psi(\tilde{t}, \rho)$ to the Dirac equation on the Rindler metric, we have $\psi(\tilde{t}, \rho) = e^{-i\epsilon_k \tilde{t}} \psi_{\epsilon_k}(\rho)$, where

$$\psi_{\epsilon_k}(\rho) = \frac{1}{\sqrt{2\pi|\kappa|}} \begin{pmatrix} \rho^{\frac{i\epsilon_k}{\kappa} - \frac{1}{2}} \\ \rho^{-\frac{i\epsilon_k}{\kappa} - \frac{1}{2}} \end{pmatrix}. \quad (\text{B.22})$$

This solution, however, is not unique. For instance, $\psi_{\epsilon_k}(\rho)$ can be expressed as the linear combination of two orthonormal spinors $\psi_{\epsilon_k}^\pm(\rho) = \mathcal{N} \rho^{\pm \frac{i\epsilon_k}{\kappa} - \frac{1}{2}} u_\pm$, where u_\pm are the eigenvectors of σ^z with eigenvalues ± 1 , respectively, which are also solutions to the Dirac equation and satisfy the eigenvalue equation $h_R \psi_{\epsilon_k}^\pm(\rho) = \epsilon_k \psi_{\epsilon_k}^\pm(\rho)$. Additionally, as we are considering a complex spinor field, there exists a further solution $\phi(\tilde{t}, \rho) = C \psi^*(\tilde{t}, \rho) = e^{i\epsilon_k \tilde{t}} \phi_{\epsilon_k}(\rho)$ to the Dirac equation [65], which satisfies the eigenvalue equation $h_R \phi_{\epsilon_k}(\rho) = -\epsilon_k \phi_{\epsilon_k}(\rho)$ and the orthonormality condition $\langle \phi_{\epsilon_k}, \psi_{\epsilon_k} \rangle = 0$. Here, C is a charge conjugation operator, defined as $C^\dagger h_R C = -h_R^*$, and $\phi(\tilde{t}, \rho)$ is the charge conjugate spinor of $\psi(\tilde{t}, \rho)$ [65]. In the chiral representation, $C = \mathbb{1}$, hence $\phi_{\epsilon_k}(\rho) = \psi_{\epsilon_k}^*(\rho)$. Analogous to $\psi_{\epsilon_k}(\rho)$, $\phi_{\epsilon_k}(\rho)$ can be expressed via a linear combination of two orthonormal spinors $\varphi_{\epsilon_k}^\pm(\rho) = \mathcal{N} \rho^{\mp \frac{i\epsilon_k}{\kappa} - \frac{1}{2}} u_\pm$ that solve the Dirac equation and satisfy the eigenvalue equation $h_R \varphi_{\epsilon_k}^\pm(\rho) = -\epsilon_k \varphi_{\epsilon_k}^\pm(\rho)$. Thus, a general solution to the Dirac equation must be constructed with both $\psi_{\epsilon_k}(\rho)$ and $\phi_{\epsilon_k}(\rho)$ via an eigenfunction decomposition.

Assuming that the orthonormal basis formed by the eigenfunctions $\psi_{\epsilon_k}(\rho)$ of the Hermitian operator h_R is complete, any function $F(\rho)$ within the Hilbert space \mathcal{H}_R defined by the inner product of Eq. (B.19) can be decomposed into a continuous sum of the eigenfunctions $\psi_{\epsilon_k}(\rho)$ as [61, 72, 73]

$$F(\rho) = \int d\mu(k) \tilde{f}(k) \psi_{\epsilon_k}(\rho), \quad (\text{B.23})$$

where $d\mu(k) = dk$ is an integration measure of the continuous index k that defines the inner product

$$\langle \tilde{f}(k), \tilde{g}(k) \rangle = \int d\mu(k) \tilde{f}^\dagger(k) \tilde{g}(k) \quad (\text{B.24})$$

of a corresponding Hilbert space $\mathcal{L}^2(k)$ of functions $\tilde{f}(k)$, which is related to \mathcal{H}_R via the eigenfunction decomposition of Eq. (B.23) and its inverse [61, 72, 73]

$$\tilde{f}(k) = \int d\mu(\rho) \psi_{\epsilon_k}^\dagger(\rho) F(\rho). \quad (\text{B.25})$$

For a consistent correspondence between the two Hilbert spaces via the eigenfunction decomposition and its inverse, we require the normalisation conditions $\langle \psi_{\epsilon_k}(\rho), \psi_{\epsilon_q}(\rho) \rangle = \delta(k - q)$, where $\int d\mu(q) \delta(k -$

$q)\tilde{f}(q) = \tilde{f}(k)$, and $\langle \psi_{\epsilon_k}(\rho), \psi_{\epsilon_k}(\rho') \rangle = \delta(\rho - \rho')$, where $\int d\mu(\rho')\delta(\rho - \rho')F(\rho') = F(\rho)$.

Using the eigenfunction decomposition defined in Eq. (B.23), the most general solution $\psi(\tilde{t}, \rho)$ to the Dirac equation in Rindler space-time can be decomposed into a continuous sum of the Dirac equation's spinor $\psi_{\epsilon_k}(\rho)$ and charge conjugate spinor $\phi_{\epsilon_k}(\rho)$ eigenfunctions. That is,

$$\psi(\tilde{t}, \rho) = \int_0^\infty d\mu(k) \left(\tilde{f}(k)e^{-i\epsilon_k\tilde{t}}\psi_{\epsilon_k}(\rho) + \tilde{g}(k)e^{i\epsilon_k\tilde{t}}\phi_{\epsilon_k}(\rho) \right). \quad (\text{B.26})$$

From the eigenvalue equation of Eq. (B.17), it is evident that $\psi_{\epsilon_k}(\rho)$ is a positive energy solution when $\epsilon_k > 0$ and a negative energy solution when $\epsilon_k < 0$, with the converse being true for $\phi_{\epsilon_k}(\rho)$. Thus, to ensure that the spinor $\psi_{\epsilon_k}(\rho)$ and its charge conjugate $\phi_{\epsilon_k}(\rho)$ always correspond to positive and negative energy solutions, respectively, we define

$$k = \begin{cases} \epsilon_k, & \text{if } \epsilon_k \geq 0 \\ -\epsilon_k, & \text{if } \epsilon_k < 0 \end{cases}, \text{ and } u_k = \begin{cases} u_+, & \text{if } k \geq 0 \\ u_-, & \text{if } k < 0 \end{cases}, \quad (\text{B.27})$$

such that the general solution to the Dirac equation in Eq. (B.26) can be expressed as [57, 59]

$$\psi(\tilde{t}, \rho) = \int_{-\infty}^\infty d\mu(k) \left(\tilde{f}(k)e^{-i|k|\tilde{t}}\psi_k(\rho) + \tilde{g}(k)e^{i|k|\tilde{t}}\phi_k(\rho) \right), \quad (\text{B.28})$$

and the eigenfunctions $\psi_k(\rho) = \mathcal{N}\rho^{\frac{ik}{\kappa} - \frac{1}{2}}u_k$ and $\phi_k(\rho) = \mathcal{N}\rho^{-\frac{ik}{\kappa} - \frac{1}{2}}u_k$ are always positive and negative energy solutions, respectively, satisfying the eigenvalue equations

$$\begin{aligned} h_R\psi_k(\rho) &= \begin{cases} k\psi_k(\rho), & \text{for } k \geq 0 \\ -k\psi_k(\rho), & \text{for } k < 0 \end{cases}, \\ h_R\phi_k(\rho) &= \begin{cases} -k\phi_k(\rho), & \text{for } k \geq 0 \\ k\phi_k(\rho), & \text{for } k < 0 \end{cases}. \end{aligned} \quad (\text{B.29})$$

As before, $\psi_k(\rho)$ and $\phi_k(\rho)$ satisfy the orthonormality conditions $\langle \psi_k(\rho), \psi_q(\rho) \rangle = \langle \phi_k(\rho), \phi_q(\rho) \rangle = \delta(k - q)$ and $\langle \psi_k(\rho), \phi_q(\rho) \rangle = 0$.

3 Quantum field theory of spinor in Rindler space-time

To quantise the solution of Eq. (B.28) to the Dirac equation in Rindler space-time, $\psi(\tilde{t}, \rho)$ and $\pi(\tilde{t}, \rho)$ are promoted to Hermitian operators $\hat{\psi}(\tilde{t}, \rho)$ and $\hat{\pi}(\tilde{t}, \rho)$ and required to satisfy the equal-time canonical anti-commutation relations of Eq. (A.19), where the canonical momentum conjugate to $\hat{\psi}(\tilde{t}, \rho)$ is given by $\hat{\pi}(\tilde{t}, \rho) = -\frac{i}{2}\hat{\psi}^\dagger(\tilde{t}, \rho)$ for the Rindler metric and by Eq. (A.18) for a general Riemann-Cartan space-time. In quantising the Dirac field, the functions $f(k)$ and $\tilde{g}(k)$ are also promoted to operators $\hat{f}(k)$ and $\hat{g}(k)$. Using the inverse of

the eigenfunction decomposition defined in Eq. (B.25), it can be verified that these operators can be expressed in terms of the Cauchy initial data, $\hat{\psi}(0, \rho)$ and $\hat{\pi}(0, \rho)$, as $\hat{f}(k) = \langle \hat{\psi}_k(\rho), \hat{\psi}(0, \rho) \rangle$ and $\hat{g}(k) = \langle \hat{\phi}_k(\rho), \hat{\psi}(0, \rho) \rangle$ [65]. Using these expressions and the orthonormality conditions of $\psi_k(\rho)$ and $\phi_k(\rho)$, the following anti-commutation relations can be derived: [65]

$$\begin{aligned} \{\hat{f}(k), \hat{f}^\dagger(q)\} &= \{\hat{g}(k), \hat{g}^\dagger(q)\} = \delta(k - q), \\ \{\hat{f}(k), \hat{f}(q)\} &= \{\hat{g}(k), \hat{g}(q)\} = 0, \end{aligned} \quad (\text{B.30})$$

which are those satisfied by typical creation and annihilation operators.

It can be explicitly shown that $\hat{f}(k)$ and $\hat{g}^\dagger(k)$ are creation and annihilation operators that act to raise and lower the energy of the Dirac field by discrete values. To do this, the Hamiltonian of the Dirac spinor on the Rindler space-time must be expressed in terms of $\hat{f}(k)$ and $\hat{g}^\dagger(k)$. From (A.22) for the Hamiltonian of a spinor on a stationary Riemann-Cartan space-time, the Hamiltonian of the spinor on the Rindler space-time will be

$$\hat{H} = \int d\rho \hat{\pi}(\tilde{t}, \rho) \partial_t \hat{\psi}(\tilde{t}, \rho), \quad (\text{B.31})$$

which, due to the Hamiltonian's Hermiticity, can be written as

$$\hat{H} = -\frac{i}{2} \int d\rho (\partial_t \hat{\psi}^\dagger(\tilde{t}, \rho)) \hat{\psi}(\tilde{t}, \rho). \quad (\text{B.32})$$

Substitution of Eq. (B.28) for the general solution to the Dirac equation in a Rindler space-time into the above Hamiltonian, and making use of the orthonormality conditions of $\psi_k(\rho)$ and $\phi_k(\rho)$, yields [65]

$$\hat{H} = \frac{|k|}{2} \int d\mu(k) \left(\hat{f}^\dagger(k)\hat{f}(k) - \hat{g}^\dagger(k)\hat{g}(k) \right). \quad (\text{B.33})$$

From this Hamiltonian and the anti-commutation relations of the operators $\hat{f}(k)$ and $\hat{g}(k)$ given in Eq. (B.30), the following commutation relations between $\hat{f}(k)$, $\hat{g}(k)$ and the Hamiltonian can be obtained:

$$[\hat{H}, \hat{f}^\dagger(k)] = \frac{|k|}{2}\hat{f}^\dagger(k), \quad [\hat{H}, \hat{f}(k)] = -\frac{|k|}{2}\hat{f}(k), \quad (\text{B.34})$$

$$[\hat{H}, \hat{g}^\dagger(k)] = -\frac{|k|}{2}\hat{g}^\dagger(k), \quad [\hat{H}, \hat{g}(k)] = \frac{|k|}{2}\hat{g}(k), \quad (\text{B.35})$$

which, in conjunction with the eigenvalue equations of $\psi_k(k)$ and $\phi_k(k)$ given in Eq. (B.29), can be used to deduce that $\hat{f}^\dagger(k)$ and $\hat{f}(k)$ are operators that act to raise and lower the energy of the quantum field by creating and annihilating quanta ψ_k of energy $|k|/2$, respectively, whilst $\hat{g}^\dagger(k)$ and $\hat{g}(k)$ act to lower and raise the energy of the quantum field by creating and annihilating quanta ϕ_k of energy $-|k|/2$, respectively. To be in line with standard notation, we re-label $\hat{f}^\dagger(k), \hat{f}(k) \mapsto \hat{a}_k^\dagger, \hat{a}_k$, and

$\hat{g}^\dagger(k), \hat{g}(k) \mapsto \hat{b}_k, \hat{b}_k^\dagger$. Therefore, the general solution to the Dirac equation in Rindler space-time is [57, 59]

$$\hat{\psi}(\tilde{t}, \rho) = \int_{-\infty}^{\infty} d\mu(k) \left(\hat{a}_k e^{-i|k|\tilde{t}} \psi_k(\rho) + \hat{b}_k^\dagger e^{i|k|\tilde{t}} \phi_k(\rho) \right), \quad (\text{B.36})$$

where $\hat{a}_k = \langle \psi_k(\rho), \psi(0, \rho) \rangle$, $\hat{b}_k^\dagger = \langle \phi_k(\rho), \psi(0, \rho) \rangle$, and $\{\hat{a}_k, \hat{a}_q^\dagger\} = \{\hat{b}_k, \hat{b}_q^\dagger\} = \delta(k - q)$, whilst all other anti-commutation relations vanish.

4 Quantum field theory of spinor in Minkowski space-time

To derive the Fulling-Davies-Unruh effect for a Rindler observer near the event horizon of the black hole, we are concerned with determining the vacuum expectation value of the Minkowski vacuum as seen by the Rindler observer [66]. Therefore, a general solution to the Minkowski space-time Dirac equation must also be obtained, and a quantum field theory for a spinor in a Minkowski space-time constructed. In (1+1)-dimensions, the Minkowski metric line element is

$$ds^2 = dT^2 - dX^2, \quad (\text{B.37})$$

where the Minkowski coordinates $X^\mu = (T, X)$ are related to the Rindler coordinates $x_R^\mu = (\tilde{t}, \rho)$ via

$$T = \rho \sinh(\kappa \tilde{t}), \quad X = \rho \cosh(\kappa \tilde{t}). \quad (\text{B.38})$$

In Minkowski space-time, as the zweibein is trivially given by $e_\mu^a = \mathbb{1}$, the Dirac equation, as is given in Eq. (B.14), simplifies to

$$(i\gamma^a e_a^\mu \partial_\mu - m) \Psi(T, X) = 0 \quad (\text{B.39})$$

for the two-component spinor $\Psi(T, X)$. Analogous to the Rindler metric, as the Minkowski metric is stationary with respect to the Minkowski time coordinate T , the vector $K^\mu = \delta_T^\mu$ (or equivalently ∂_T) is a Killing vector that is time-like for all of the Minkowski space-time. Thus, the energy E of the spinor is a well-defined quantity that is conserved along the Minkowski metric's geodesics [28, 65], and the Dirac equation can be solved via the separation of variables

$$\Psi(T, X) = e^{-iE_K T} \Psi_{E_K}(X), \quad (\text{B.40})$$

where $\Psi_{E_K}(X) = (\Psi_{E_K}^+(X) \ \Psi_{E_K}^-(X))^T$ is a two-component spinor that depends only on X . Therefore, the Minkowski space-time Dirac equation can be expressed as the following eigenvalue equation:

$$h_M \Psi_{E_K}(X) = E_K \Psi_{E_K}(X), \quad (\text{B.41})$$

where $h_M = i\gamma^0 \gamma^1 \partial_X + m\gamma^0$ is a linear differential operator that is Hermitian under the conserved inner product

$$\langle \Phi(X), \Psi(X) \rangle = \int d\mu(X) \Phi^\dagger(X) \Psi(X), \quad (\text{B.42})$$

and $d\mu(X) = dX$ is a measure of integration. That is, h_M satisfies $\langle \Phi, h_M \Psi \rangle = \langle h_M \Phi, \Psi \rangle$ [73]. Once again restricting ourselves to the case of a massless spinor and choosing the chiral representation of the γ matrices, the Hermitian operator h_M can be expressed as $h_M = -u\sigma^z \partial_X \Psi_{E_K}(X)$. Therefore, the eigenvalue equation corresponds to the two following decoupled differential equations:

$$E_K \Psi_{E_K}^\pm(X) \pm i\partial_X \Psi_{E_K}^\pm(x) = 0, \quad (\text{B.43})$$

where $\Psi_{E_K}^\pm(x)$ denote the components of the spinor $\Psi_{E_K}(x)$ that have the solutions $\Psi_{E_K}^\pm(X) = \mathcal{N} e^{\pm iE_K X}$, where $\mathcal{N} = 1/\sqrt{2\pi}$ is a normalisation constant chosen such that $\langle \Psi_{E_K}(X), \Psi_{E_Q}(X) \rangle = \delta(K - Q)$. Hence, as a solution to the Dirac equation in Minkowski space-time, we have

$$\Psi(T, X) = \frac{1}{\sqrt{2\pi}} e^{-iE_K T} \begin{pmatrix} e^{iE_K X} \\ e^{-iE_K X} \end{pmatrix} \quad (\text{B.44})$$

The charge conjugate solution $\Phi(T, X) = C\Psi^*(T, X) = e^{iET} \Phi_{E_K}(X)$ to the Minkowski space-time Dirac equation, which satisfies the eigenvalue equation $h_M \Phi_{E_K}(x) = -E_K \Phi_{E_K}(X)$ and the orthonormality condition $\langle \Phi_{E_K}, \Psi_{E_K} \rangle = 0$, will be given by $\Phi(T, X) = \Psi^*(T, X)$.

Again, assuming that the orthonormal basis formed by the eigenfunctions $\Psi_{E_K}(X)$ of the Hamiltonian h_M is complete, any function $F(X)$ within the Hilbert space \mathcal{H}_M defined by the conserved inner product of Eq. (B.42) can be decomposed into a continuous sum of eigenfunctions $\Psi_{E_K}(X)$ as [61, 72, 73]

$$F(X) = \int d\mu(K) \tilde{f}(K) \Psi_{E_K}(X), \quad (\text{B.45})$$

where $d\mu(K) = dK$ is an integration measure of the continuous index K that defines the conserved inner product

$$\langle \tilde{f}(K), \tilde{g}(K) \rangle = \int \mu(K) \tilde{f}^\dagger(K) \tilde{g}(K), \quad (\text{B.46})$$

of a corresponding Hilbert space $\mathcal{L}^2(K)$ of functions $\tilde{f}(K)$, which is related to \mathcal{H}_M via the eigenfunction decomposition of Eq. (B.45) and its inverse [61, 72, 73]

$$\tilde{f}(K) = \int d\mu(X) \Psi_{E_K}^\dagger(X) F(X). \quad (\text{B.47})$$

To consistently relate the two Hilbert spaces via the eigenfunction decomposition and its inverse, we require the normalisation conditions $\langle \Psi_{E_K}(X), \Psi_Q(X) \rangle = \delta(K - Q)$, where $\int d\mu(Q) \delta(K - Q) \tilde{f}(Q) = \tilde{f}(K)$, and $\langle \Psi_{E_K}(X), \Psi_{E_K}(X') \rangle = \delta(X - X')$, where $\int d\mu(X') \delta(X - X') F(X') = F(X)$ [61, 72, 73].

As in the Rindler case, from the eigenfunction decomposition of Eq. (B.45), the most general solution $\Psi(T, X)$ of the Minkowski space-time Dirac equation can be decomposed into a continuous sum of the Dirac equation's

spinor $\Psi_{E_K}(X)$ and charge conjugate spinor $\Phi_{E_K}(X)$ eigenfunctions. That is,

$$\Psi(T, X) = \int_{-\infty}^{\infty} d\mu(K) \left(\tilde{f}(K) e^{-i|K|T} \Psi_K(X) + \tilde{g}(K) e^{i|K|T} \Phi_K(X) \right), \quad (\text{B.48})$$

where, to once again ensure that the spinor Ψ_{E_K} and its charge conjugate Φ_{E_K} always correspond to positive and negative energy solutions, respectively, we have defined

$$K = \begin{cases} E_K, & \text{if } E_K \geq 0 \\ -E_K, & \text{if } E_K < 0 \end{cases}, \quad u_K = \begin{cases} u_+, & \text{if } K \geq 0 \\ u_-, & \text{if } K < 0 \end{cases} \quad (\text{B.49})$$

and the eigenfunctions $\Psi_K(X) = \mathcal{N} e^{-iKX} u_K$ and $\Phi_K(X) = \mathcal{N} e^{iKX} u_K$.

Once again, this solution to the Dirac equation for a spinor in Minkowski space-time can be quantised by promoting $\Psi(T, X)$ and $\Pi(T, X) = -\frac{i}{2} \Psi^\dagger(T, X)$ to Hermitian operators and imposing the equal-time canonical anti-commutations of Eq. (A.19). In quantising the Dirac field in Minkowski space-time, the functions $\tilde{f}(K)$ and $\tilde{g}(K)$ are promoted to the operators $\hat{f}(K)$ and $\hat{g}(K)$, respectively. Using the inverse eigenfunction decomposition defined in (B.47), it can be verified that the operators $\hat{f}(K)$ and $\hat{g}(K)$ can be expressed in terms of the Cauchy initial data, $\hat{\Psi}(0, X)$ and $\hat{\Pi}(0, X)$, as $\hat{f}(K) = \langle \hat{\Psi}_K(X), \hat{\Psi}(0, X) \rangle$ and $\hat{g}(K) = \langle \hat{\Phi}_K(X), \hat{\Psi}(0, X) \rangle$. From these expressions and the orthonormality conditions of $\hat{\Psi}_K(X)$ and $\hat{\Phi}_K(X)$, the following anti-commutation relations can be derived [65]:

$$\{\hat{f}(K), \hat{f}^\dagger(Q)\} = \{\hat{g}(K), \hat{g}^\dagger(Q)\} = \delta(K - Q), \quad (\text{B.50})$$

$$\{\hat{f}(K), \hat{f}(Q)\} = \{\hat{g}(K), \hat{g}^\dagger(Q)\} = 0, \quad (\text{B.51})$$

which are the anti-commutation relations satisfied by typical creation and annihilation operators.

Analogous to the Rindler space-time case, it then follows that $\hat{f}^\dagger(K)$ and $\hat{g}(K)$ are operators that act to raise and lower the energy of the quantum field by creating and annihilating quanta Ψ_K of energy $|K|/2$, respectively, whilst $\hat{g}^\dagger(K)$ and $\hat{f}(K)$ are operators that act to lower and raise the energy of the quantum field by creating and annihilating quanta Φ_K of energy $-|K|/2$, respectively. Thus, after re-labelling $\hat{f}(K), \hat{f}^\dagger(K) \mapsto \hat{A}^\dagger(K), \hat{A}_K$, and $\hat{g}^\dagger(K), \hat{g}(K) \mapsto \hat{B}_K, \hat{B}_K^\dagger$, the general solution to the Dirac equation in Minkowski space-time is [57]

$$\hat{\Psi}(T, X) = \int_{-\infty}^{\infty} d\mu(K) \left(\hat{A}_K e^{-i|K|T} \Psi_K(X) + \hat{B}_K^\dagger e^{i|K|T} \Phi_K(X) \right), \quad (\text{B.52})$$

where $\hat{A}_K = \langle \Psi_K, \Psi(0, X) \rangle$, $\hat{B}_K^\dagger = \langle \Phi_K, \Psi(0, X) \rangle$, and $\{\hat{A}_K, \hat{A}_Q^\dagger\} = \{\hat{B}_K, \hat{B}_Q^\dagger\} = \delta(K - Q)$, whilst all other anti-commutation relations vanish.

5 Bogoliubov transformation and Hawking effect

The Fulling-Davies-Unruh effect originates in the fact that the vacuum states of a Minkowski observer and a Rindler observer are not equivalent [4, 63]. An observer in a Minkowski space-time will define their vacuum state as the state $|0_M\rangle$ that satisfies $\hat{A}_K|0_M\rangle = \hat{B}_K|0_M\rangle = 0 \forall K$, where \hat{A}_K and \hat{B}_K are the particle and anti-particle annihilation operators, respectively, associated with the general solution of Eq. (B.52). On the other hand, a Rindler observer will define their vacuum state as the state $|0_R\rangle$ that satisfies $\hat{a}_k|0_R\rangle = \hat{b}_k|0_R\rangle = 0 \forall k$, where \hat{a}_k and \hat{b}_k are the particle and anti-particle annihilation operators, respectively, associated with the general solution of Eq. (B.36). Generally, the vacuum states $|0_M\rangle$ and $|0_R\rangle$ are not equivalent, as the quantum field theories for the Minkowski and Rindler observers have been constructed by quantising general solutions to the Dirac equation that were obtained for different coordinate systems. Nevertheless, the two quantum field theories should be equivalent when the Minkowski and Rindler coordinate systems are equivalent [61, 72]. This occurs at $\tilde{t} = T = 0, \rho = X$; thus, at $\tilde{t} = T = 0$, we have $\hat{\psi}(0, \rho) = \hat{\Psi}(0, X)$ and $\hat{\pi}(0, \rho) = \hat{\Pi}(0, X)$ [61]. As the creation and annihilation operators are determined by each theory's Cauchy initial data $\hat{\psi}(0, \rho)$ and $\hat{\Psi}(0, X)$, their equivalence at $\tilde{t} = T = 0$ allows each theory's creation and annihilation operators to be expressed in terms of the other's. That is,

$$\begin{aligned} \hat{a}_k &= \langle \hat{\psi}_k, \hat{\psi}(0, \rho) \rangle \\ &= \int d\mu(K) \left(\hat{A}_K \langle \hat{\psi}_k, \hat{\Psi}_K \rangle + \hat{B}_K^\dagger \langle \hat{\psi}_k, \hat{\Phi}_K \rangle \right) \end{aligned} \quad (\text{B.53})$$

and

$$\begin{aligned} \hat{b}_k^\dagger &= \langle \hat{\phi}_k, \hat{\psi}(0, \rho) \rangle \\ &= \int d\mu(K) \left(\hat{A}_K \langle \hat{\phi}_k, \hat{\Psi}_K \rangle + \hat{B}_K^\dagger \langle \hat{\phi}_k, \hat{\Phi}_K \rangle \right), \end{aligned} \quad (\text{B.54})$$

where the equivalence of the two integration measures $d\mu(\rho)$ and $d\mu(X)$ at $\tilde{t} = T = 0$ is used to compute the inner product between the Minkowski and Rindler eigenstates. Eqs. (B.53) and (B.54) each give a Bogoliubov transformation between the Minkowski and Rindler creation and annihilation operators [57, 59, 61]. Using these Bogoliubov transformations and the fact that $\hat{A}_K|0_M\rangle = \langle 0_M|\hat{A}_K^\dagger = 0$, the vacuum expectation value of the Minkowski vacuum, as seen by the Rindler observer, can be expressed as

$$\langle 0_M|\hat{a}_k^\dagger \hat{a}_q|0_M\rangle = \int d\mu(K) \langle \hat{\phi}_k, \hat{\Psi}_K \rangle \langle \hat{\psi}_q, \hat{\Phi}_K \rangle, \quad (\text{B.55})$$

where the inner products, $\langle \hat{\phi}_k, \hat{\Psi}_K \rangle$ and $\langle \hat{\psi}_q, \hat{\Phi}_K \rangle$, can be explicitly calculated as follows: [57]

$$\begin{aligned} \langle \hat{\psi}_q, \hat{\Phi}_K \rangle &= \frac{u_q^T u_K}{2\pi\sqrt{|\kappa|}} \int_0^\infty dX \left(X^{-\frac{iq}{\kappa} - \frac{1}{2}} e^{-iKX} \right), \quad (\text{B.56}) \\ &= \frac{\delta_{qK}}{2\pi\sqrt{|\kappa|}} e^{-\frac{\pi q}{2\kappa} - \frac{i\pi}{4}} K^{\frac{iq}{\kappa} - \frac{1}{2}} \Gamma\left(\frac{1}{2} - \frac{iq}{\kappa}\right), \end{aligned} \quad (\text{B.57})$$

where denotes the $\Gamma(z)$ is the gamma function and, in the final equality, the identity $i = e^{\frac{i\pi}{2}}$ was used;

$$\begin{aligned} \langle \hat{\phi}_k, \hat{\Psi}_K \rangle &= \frac{u_k^T u_K}{2\pi\sqrt{|\kappa|}} \int_0^\infty dX \left(X^{\frac{ik}{\kappa} - \frac{1}{2}} e^{iXK} \right), \quad (\text{B.58}) \\ &= \frac{\delta_{kK}}{2\pi\sqrt{|\kappa|}} e^{-\frac{\pi k}{2\kappa} + \frac{i\pi}{4}} K^{-\frac{ik}{\kappa} + \frac{1}{2}} \Gamma^*\left(\frac{1}{2} - \frac{ik}{\kappa}\right), \end{aligned} \quad (\text{B.59})$$

where $\Gamma^*(z) = \Gamma(z^*)$ and, in the final equality, the identity $-i = e^{-\frac{i\pi}{2}}$ was used. Hence, the vacuum expectation value of the Minkowski vacuum, as seen by the Rindler observer, can be found to be

$$\begin{aligned} \langle 0_M | \hat{a}_k^\dagger \hat{a}_q | 0_M \rangle &= \frac{\delta_{kq}}{2\pi} e^{-\frac{\pi}{2\kappa}(k+q)} \Gamma^*\left(\frac{1}{2} - \frac{ik}{\kappa}\right) \\ &\quad \Gamma\left(\frac{1}{2} - \frac{iq}{\kappa}\right) \delta(k-q), \end{aligned} \quad (\text{B.60})$$

$$\langle 0_M | \hat{a}_k^\dagger \hat{a}_k | 0_M \rangle = \frac{\delta(0)}{2} e^{-\frac{\pi k}{\kappa}} \operatorname{sech}\left(\frac{\pi k}{\kappa}\right), \quad (\text{B.61})$$

$$= \frac{\delta(0)}{e^{2\pi k/\kappa} + 1}, \quad (\text{B.62})$$

where, in the second equality, the identity $|\Gamma(ix + \frac{1}{2})|^2 = \pi \operatorname{sech}(\pi x)$ has been used. Eq. (B.62) for the Minkowski

vacuum expectation value, as seen by the Rindler observer, is a Fermi-Dirac distribution for fermions in thermal equilibrium with a temperature $T_H = \kappa/2\pi$. That is, an observer accelerating with a constant proper acceleration κ will experience their vacuum state to be populated by thermal radiation with a temperature T_H [61–63]; this is the Fulling-Davies-Unruh effect. As the Schwarzschild metric can be approximated by the Rindler metric near the event horizon, an observer near the event horizon of a Schwarzschild black hole will experience the Fulling-Davies-Unruh effect [4, 69].

Appendix C. Fermion zero-mode entropy of (1+1)D black hole exterior

In this appendix, we extend the analysis of Sec. III to derive the fermion zero-mode entropy of both the black hole's interior and exterior regions. This derivation is analogous to that of Sec. III and involves determining the density of states of Eq. (12) for both the interior region, which is bound by $[a_c, x_h - a_c]$, and a portion of the exterior space-time, which we take to be bound by $[x_h + a_c, s]$, where $s \geq x_h + a_c$. To prevent an infinite number of degrees of freedom, from points on either side of the event horizon with a separation of less than a_c , from contributing to the density of states, the lower limit of s has been restricted to a distance a_c from the event horizon [38, 51, 52].

Taking the sub-luminal dispersion relation of Eq. (5), and considering the emergence of the two zero-modes at momenta p_\pm in the interior region, along with the zero-mode at p_0 that exists throughout the entire space-time, the density of states of Eq. (11) for the interior and exterior regions will be given by

$$N(0) = \frac{N_F}{2\pi\hbar} \int_{a_c}^{x_h - a_c} dx \left(\frac{1}{|1-v(x)|} + \left| \frac{1}{(1-v(x))} - \frac{1}{(1+v(x))} \right| \right) + \frac{\tilde{N}_F}{2\pi\hbar} \int_{x_h + a_c}^s dx \left(\frac{1}{|1-v(x)|} \right), \quad (\text{C.1})$$

where \tilde{N}_F denotes the integer number of massless fermionic fields in the exterior region. Taking the coupling $v(x) = \sqrt{x_h/x}$ that corresponds to the space-time of a Schwarzschild black hole, and working in the limit $0 < a_c \ll x_h$, this density of states can be solved to yield

$$N(0) = \frac{N_F x_h}{\pi\hbar} \left(2 \ln\left(\frac{2x_h}{a_c}\right) + \ln(2) - \frac{7}{2} \right) + \frac{\tilde{N}_F x_h}{\pi\hbar} \left(\frac{1}{2} \left(\frac{s}{x_h} \right) + \left(\frac{s}{x_h} \right)^{\frac{1}{2}} + \ln\left|s^{\frac{1}{2}} - x_h^{\frac{1}{2}}\right| + \ln\left(\frac{2x_h^{\frac{1}{2}}}{a_c}\right) - \frac{3}{2} \right), \quad (\text{C.2})$$

where the term preceded by N_F corresponds to the density of states of the entire black hole interior, and the term preceded by \tilde{N}_F the density of states of the black hole exterior.

Assuming that the fermions in the black hole's interior and exterior regions are well described by a thermal Gibbs state, their thermal energy and entropy can be defined by Eqs. (15) and (16), respectively. Once again, further assuming that the temperature associated with this thermal state is the Hawking temperature of Eq. (17), the fermion zero-mode entropy of the black hole's interior and exterior will be given by

$$\mathcal{S}(T_H) = \frac{N_F}{6} \ln\left(\frac{2x_h}{a_c}\right) + \frac{\tilde{N}_F}{12} \left(\frac{1}{2} \left(\frac{s}{x_h} \right) + \left(\frac{s}{x_h} \right)^{\frac{1}{2}} + \ln\left(\frac{2x_h^{\frac{1}{2}}}{a_c}\right) + \ln\left|s^{\frac{1}{2}} - x_h^{\frac{1}{2}}\right| \right) + \mathcal{S}'_0 \quad (\text{C.3})$$

where $\mathcal{S}'_0 = \mathcal{S}_0 - 3\tilde{N}_F/24$. For the case where $s = x_h + a_c$, and in the limit $a_c \ll x_h$, Eq. (C.3) for the fermion zero-mode entropy of the black hole's interior and exterior reduces to Eq. (19), as expected.

Appendix D. Conformal Invariance of Lattice Simulator

In this appendix, we study the correspondence between a transformation of the mean-field Hamiltonian and a change in coordinates of the continuum limit Hamiltonian. This correspondence arises due to an equivalence between the choice of spinor renormalisation and a conformal scaling of the emergent metric. In the continuum limit, this transformation preserves the curvature of the underlying space-time; thus, scalar invariant quantities remain unchanged.

In deriving the continuum limit of the mean-field Hamiltonian of Eq. (2), the choice of zweibein defined by Eq. (9) is not unique. One could alternatively define another set of coefficients \tilde{e}_a^μ that are related to e_a^μ via the transformation $e_a^\mu = C(u, v)\tilde{e}_a^\mu$, where, as we will see, $C(u, v)$ is a conformal scale factor. Following this transformation, the mean-field continuum limit Hamiltonian of Eq. (7) can be expressed as

$$H = \int dp C(u, v) \chi^\dagger(p) \tilde{e}_a^x \alpha^a p \chi(p), \quad (\text{D.4})$$

which, following an inverse Fourier transformation and, subsequently, a Legendre transformation, can be used to obtain the action

$$S = i \int d^{1+1}x |\tilde{e}| \bar{\varphi}(x) \tilde{e}_a^\mu \gamma^a \overleftrightarrow{\partial}_\mu \varphi(x). \quad (\text{D.5})$$

Here, the curved space-time spinor φ , which is related to the lattice spinor χ via the renormalisation $\chi = \sqrt{|\tilde{e}|/C} \varphi$ and satisfies the anti-commutation relations of Eq. (A.20), and its conjugate $\bar{\varphi} = \varphi^\dagger(x) \gamma^0$, have been defined.

The action of Eq. (D.5) is, once again, that of a massless Dirac spinor φ propagating freely on a (1+1)-dimensional Riemann-Cartan space-time, with the zweibein \tilde{e}_a^μ corresponding to the space-time metric line element

$$d\tilde{s}^2 = C(u, v)^2 \left[\left(1 - \frac{v^2}{u^2}\right) dt^2 - \frac{2v}{u^2} dt dx - \frac{dx^2}{u^2} \right]. \quad (\text{D.6})$$

From the line element of Eq. (D.6), we see that $C(u, v)$ is a conformal scale factor that relates the Gullstrand-Painlevé line element of Eq. (10) to that of Eq. (D.6) via the conformal transformation $d\tilde{s}^2 = C(u, v)^2 ds^2$.

A unique case of the general curved space-time of Eq. (D.6) can be obtained by taking $C(u) = \sqrt{u(x)}$ and working in the limit where $v \rightarrow 0$. In this case, the line element of Eq. (D.6) reduces to

$$d\tilde{s}^2 = u(x) dt^2 - \frac{dx^2}{u(x)}, \quad (\text{D.7})$$

which is that of the (1+1)-dimensional Schwarzschild metric. In this case, the corresponding lattice Hamiltonian is that of Eq. (2) with a position-dependent nearest-neighbour coupling $u(x)$ and vanishing chirality term.

To illustrate the invariance of the space-time's curvature under this conformal transformation, it is instructive to study the Ricci curvature scalar R , defined as $R = g^{\mu\nu} R_{\mu\nu}$, where $R_{\mu\nu} = R^\lambda_{\mu\lambda\nu}$ denotes the Ricci tensor, which is itself defined in terms of the Riemann tensor $R_{\alpha\mu\lambda\nu}$. In a local inertial reference frame, the Riemann tensor is given by [66]

$$R_{\alpha\mu\lambda\nu} = \frac{1}{2} (g_{\alpha\nu, \mu\lambda} - g_{\alpha\lambda, \mu\nu} + g_{\mu\lambda, \alpha\nu} - g_{\mu\nu, \alpha\lambda}), \quad (\text{D.8})$$

thus, for a stationary (1+1)-dimensional space-time metric, the components of the Ricci tensor can be found to be $R_{tt} = -\frac{1}{2} g^{xx} g_{tt, xx}$, $R_{xt} = R_{tx} = \frac{1}{2} g^{xt} g_{tt, xx}$, and $R_{xx} = -\frac{1}{2} g^{tt} g_{tt, xx}$. For the space-time metric of Eq. (D.6), the Ricci scalar is, therefore, given by

$$R = \frac{u(x)^2}{C(x)^4} \frac{d^2}{dx^2} \left[C(x)^2 \left(1 - \frac{v(x)^2}{u(x)^2} \right) \right]. \quad (\text{D.9})$$

It can be verified from the Ricci scalar of Eq. (D.9) that the curvature remains invariant under the conformal transformation and renormalisation of the curved space-time spinor, provided that the couplings are transformed such that they correspond to the same space-time geometry. Take, for example, the limit where the line element of Eq. (D.6) reduces to the Gullstrand-Painlevé line element of Eq. (10). In this limit, and for the couplings corresponding to the geometry of a (1+1)-dimensional Schwarzschild black hole, $u = 1$ and $v(x) = \sqrt{x_h/x}$, the Ricci scalar is $R = -2x_h/x^3$. This is equivalent to the value obtained in the limit where the line element of Eq. (D.6) reduces to the Schwarzschild metric of Eq. (D.7) with the couplings of the (1+1)-dimensional Schwarzschild black hole geometry, $u(x) = (1 - x_h/x)$ and $v = 0$.